https://dx.doi.org/10.1016/j.bioorg.2023.106983

Sulfonamidyl Derivatives of Sigmacidin: Protein-Protein Interaction Inhibitors Targeting Bacterial RNA Polymerase and Sigma Factor Interaction Exhibiting Antimicrobial Activity against Antibiotic-Resistant Bacteria

Jiqing Ye [a,b,1], *Cheuk Hei Kan* [c,1], *Yingbo Zheng* [a], *Tsz Fung Tsang* [c], *Adrian Jun Chu* [c], *King Hong Chan* [a], *Xiao Yang* [c,*], *Cong Ma* [a,*]

[a] State Key Laboratory of Chemical Biology and Drug Discovery, Department of Applied Biology and Chemical Technology, The Hong Kong Polytechnic University, Hung Hom, Kowloon, Hong Kong SAR, China

[b] School of Pharmacy, Inflammation and Immune Mediated Diseases Laboratory of Anhui Province, Anhui Medical University, Hefei, China

[c] Department of Microbiology, The Chinese University of Hong Kong, Prince of Wales Hospital, Shatin, Hong Kong SAR, China

[1] Co-first authors

Abstract

RNA polymerase is an essential enzyme involved in bacterial transcription, playing a crucial role in RNA synthesis. However, it requires the association with sigma factors

to initiate this process. In our previous work, we utilized a structure-based drug discovery approach to create benzoyl and benzyl benzoic acid compounds. These compounds were designed based on the amino acid residues within the key binding site of sigma factors, which are crucial for their interaction with RNA polymerase. By inhibiting bacterial transcription, these compounds exhibited notable antimicrobial activity, and we coined them as sigmacidins to highlight their resemblance to sigma factors and the benzoic acid structure. In this study, we further modified the compound scaffolds and developed a series of sulfonamidyl benzoic acid derivatives. These derivatives displayed potent antimicrobial activity, with minimum inhibitory concentrations (MICs) as low as 1 μg/mL, demonstrating their efficacy against bacteria. Furthermore, these compounds demonstrated low cytotoxicity, indicating their potential as safe antimicrobial agents. To ascertain their mechanism of action in interfering with bacterial transcription, we conducted biochemical and cellular assays. Overall, this study showcases the effectiveness of sulfonamidyl benzoic acid derivatives as antimicrobial agents by targeting protein-protein interactions involving RNA polymerase and sigma factors. Their strong antimicrobial activity and low cytotoxicity implicate their potential in combating antibiotic-resistant bacteria.

Keywords: Bacterial transcription; RNA polymerase; Sigma factor; Inhibitor; Antimicrobial

1. Introduction

Bacterial transcription is a valid yet underutilized target for antimicrobial agent discovery [1]. Presently, the options for interfering with this crucial process are limited to rifampicin and fidaxomicin, both of which target the core enzyme of RNA polymerase (RNAP) [1]. However, the flexible nature of RNAP increases the likelihood of antimicrobial resistance (AMR) emergence after treatment of these drugs [2, 3], hindering the development of other natural products as bacterial transcription inhibitors.

Bacterial transcription is regulated by numbers of small proteins namely transcription factors [4]. They bind to RNAP to form diverse transcription complexes for regulating RNA synthesis. Therefore, targeting the protein-protein interactions (PPIs) in bacterial transcription may inhibit this essential biological process and provide a solution for novel antibiotic discovery [1].

In the past, PPI was considered undruggable due to the challenge of designing a small molecule to target the large and flat interfaces of proteins. However, recent advancements revealed some critical binding sites on the PPI involving surface that are sufficiently small and appropriate for drug design [5]. Some PPI inhibitors have therefore been discovered as antimicrobials [6], making PPIs in bacterial transcription become very important for novel antimicrobial agent discovery [7]. Based on the strategy of structure-based drug design [8] and in-house developed screening assay [9], we have discovered a series of PPI inhibitors targeting bacterial transcription factors NusB and NusE [10-16].

Based on the structural information and biochemical validation, we have studied the major binding site between RNAP and the housekeeping sigma (σ) factor [17]. This σ factor, highly conserved in both Gram-positive (σ^A) and Gram-negative (σ^{70}) bacteria,

is a small protein binds to RNAP to initiate bacterial transcription by recognizing DNA promoters (Fig. 1A) [18]. In our previous studies, we have validated the important amino acids at RNAP β' subunit clamp-helix region (β'CH) for binding to σ region 2.2 (Fig. 1B) [19], followed by adopting structure-based drug design and *in silico* screening of a drug-like compound library to identify several hit compounds including **C3** [20]. Meanwhile, other RNAP-σ PPI inhibitors have also been identified [21, 22].

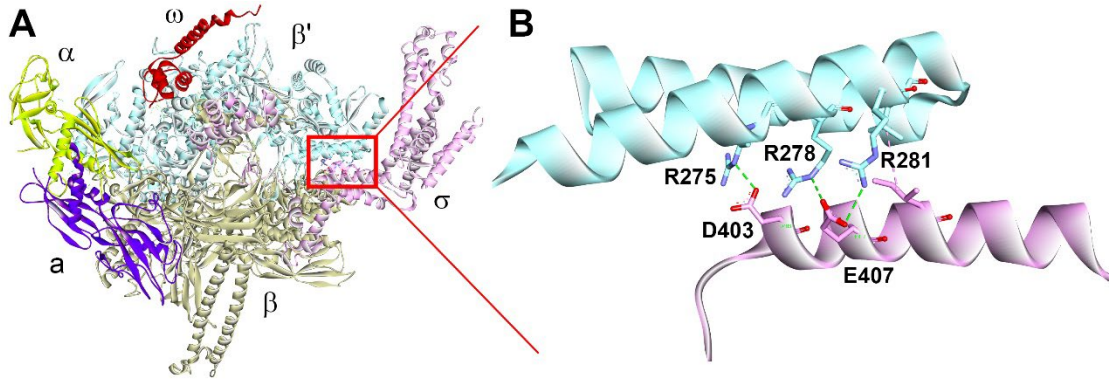

Fig. 1. Structure of **A)** the *Escherichia coli* RNAP holoenzyme crystal complex (PDB: 4LJZ [23]) and **B)** interactions at the interface of $\sigma_{2.2}$ and β'CH [17].

Following compound **C3** (Fig. 2A), structural modifications and antimicrobial activity testing have been carried out. We found that the benzoic acid moiety is the key structure for binding to β'CH and exhibiting antimicrobial activity [24-26]. Therefore, this new class of antimicrobial compounds was coined sigmacidin to address the structure-based design by mimicking the σ factor and the key structure of benzoic acid [27]. As the substituents on the left benzene ring significantly improved antimicrobial activity (**C3-005**), in this study, we focused on the modifications of the carbonyl linker of **C3-005** to the sulfonamidyl group. Given that sulfonamides are a known class of synthetic antimicrobial drugs and also commonly exist in therapeutic agents [28], we evaluated

the antimicrobial activity and its mechanism, cytotoxicity, and pharmacokinetic properties of this new series of sigmacidin derivatives to explore the potential of structural diversifications.

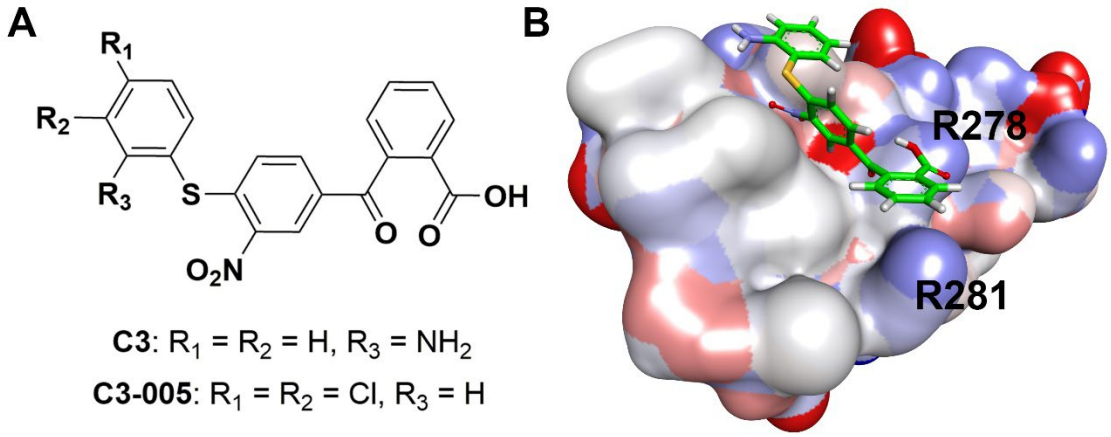

Fig. 2. **A)** Structures of **C3** and **C3-005**; **B)** Docking model of **C3** (green) to β'CH (surface view), hydrophobic: white, positive charge: blue, negative charge: red.

2. Results and discussion

2.1. Design of sulfonamidyl derivatives

In previous studies, we demonstrated that the carbonyl, methylene, and aminomethylene linker provided superior antimicrobial activity to analogues with the amide linker [24-26]. In this article, we selected the sulfonamide moiety as the linker to connect diphenylsulfide and benzoic acid to determine the structure requirement for the linker. Additionally, the pharmacophore docking model revealed that the benzoic acid moiety is clamped by β'CH R278 and R281 (Fig. 1B & 2B). Thus, we intended to design substituted benzoic acid to probe the small semi-pocket formed by β'CH for

binding and examine the effect of substitutions on benzoic acid on the antimicrobial activity.

Compared to amide, sulfonamide has a more acidic proton suitable for substitution reactions. We also intended to identify whether additional groups on sulfonamide nitrogen can be beneficial to the antimicrobial activity of new analogues and the scaffold of sigmacidin and explore the potential of scaffold diversity of sigmacidins.

2.2 Chemistry

Compounds **5a** – **5j** were synthesized as shown in **Scheme 1**. 4-Chloro-3-nitrobenzenesulfonyl chloride was condensed with corresponding amines to provide compounds **3a** – **3j** in 50 % – 75 % yield, followed by the substitution of -Cl group with 3,4-dichlorobenzenethiol to afford intermediates **4a** – **4j** in 70 % – 95 % yield. Finally, the hydrolysis of the methyl ester group provided compounds **5a** – **5j**. We synthesized **5b** at the first stage for antimicrobial activity testing to probe the substitution effect at the sulfonamide nitrogen.

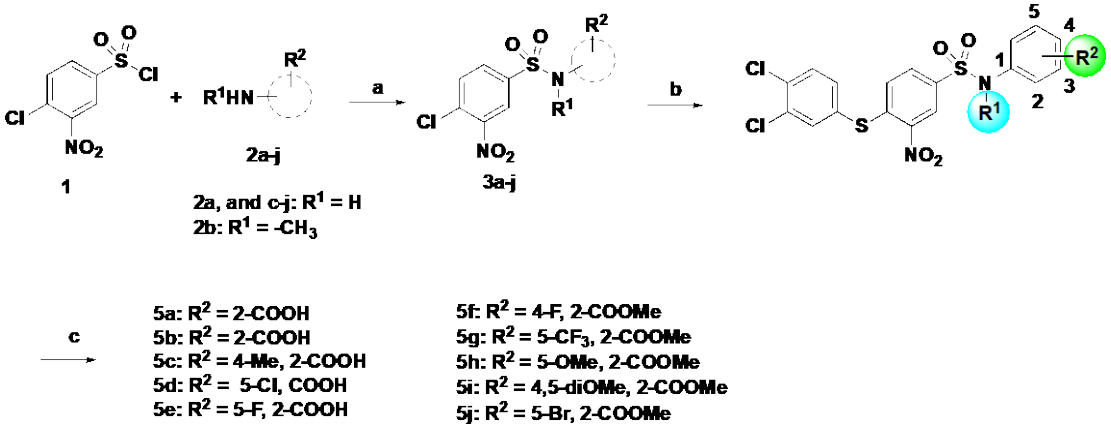

Scheme 1. Synthetic route to compounds **5a** – **5j**. Reagents and conditions: a) Anilines, pyridine, DCM, 0 °C, overnight, 50 % – 75 %; b) 3,4-dichlorobenzenethiol, NaOAc, EtOH, reflux, 6 h, 70 % – 90 %; c) NaOH, H_2O/dioxane, 50 °C, overnight.

Through a preliminary antimicrobial activity testing, we observed that compound **5b** as the methylated **5a** at sulfonamide nitrogen exhibited a reduced antibacterial activity. The result indicated that the modifications of the sulfonamide group might affect the activity. As shown in **Scheme 2**, sulfonamide intermediates **4c** – **4f** were subjected to reaction with a series of organobromides in the presence of K_2CO_3 in DMF gave **6a** – **6h** in 60 % – 90 % yield [29]. After hydrolysis of methyl esters, compounds **7a** – **7k** were obtained.

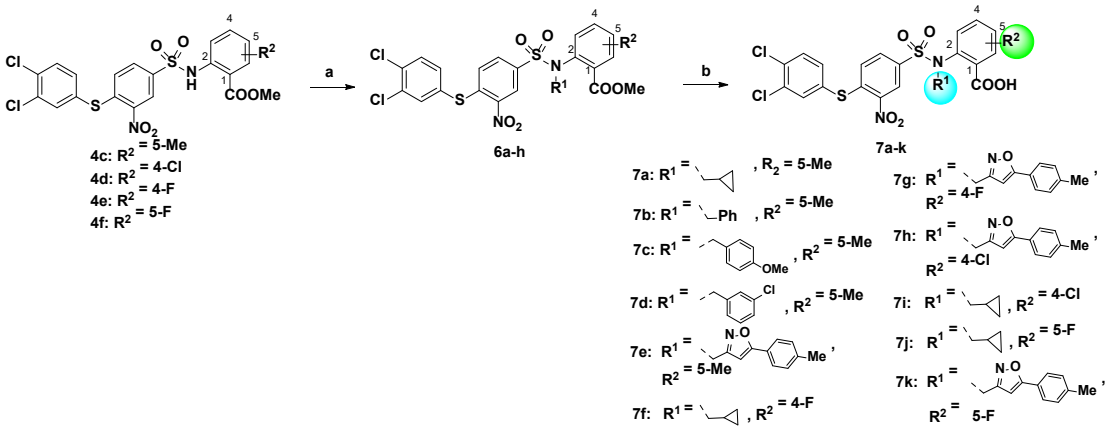

Scheme 2. Synthetic route to compounds **7a** – **7k**. Reagent and conditions: a) R^1Br, K_2CO_3, DMF, 80 °C, overnight, 60 % – 90 %; b) NaOH, H_2O/dioxane, 50 °C, overnight.

Alkylamine derivatives were also synthesized as depicted in **Scheme 3** [30]. Alkylation of **4c** with 1,4-dibromobutane in the presence of K_2CO_3 yielded compound **8** in 72 % yield, which was further aminated with various secondary amines to provide compounds **9a** – **9d**. Methyl esters were hydrolyzed to furnish *N*-alkylamines **10a** – **10d**.

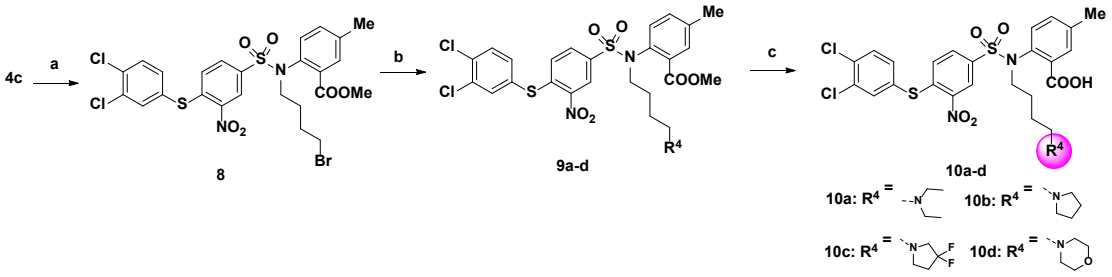

Scheme 3. Synthetic route to compounds **10a** – **10d**. Reagent and conditions: a) 1,4-Dibromobutane, K_2CO_3, DMF, 50 °C, overnight, 72 %; b) amines, K_2CO_3, DMF, 40 °C; 50 % – 90 %; c) NaOH, H_2O/dioxane, 50 °C, overnight.

2.3. Antimicrobial activity

All the synthesized compounds were subjected to antimicrobial activity testing against *Streptococcus pneumoniae* and *Staphylococcus aureus*, two of the World Health Organization (WHO) priority pathogens [31], under the Clinical and Laboratory Standards Institute (CLSI) guidelines [32]. Initially, the minimum inhibitory concentrations (MICs) of compounds **5a – 5j** were determined. Table 1 shows that **5a** demonstrated antimicrobial activity against both bacteria, in which *S. pneumoniae* was more susceptible to **5a** than *S. aureus* (MIC 2 µg/mL vs 8-16 µg/mL). This finding is

consistent with previously designed and synthesized sigmacidin compounds with carbonyl, methylenyl, aminomethylenyl linkers [24-26]. In contrast, the MICs of **5b**, featuring with the methyl substitution on the sulfonamidyl nitrogen of **5a**, reduced to 64-128 μg/mL. While leaving the sulfonamidyl nitrogen unsubstituted, **5c – 5j** maintained or improved against some or all the bacteria tested, regardless of whether electron-withdrawing or -donating substituents were present. These results differed from previous results that electron-donating groups on the right benzene ring reduced antimicrobial activity, whereas electron-withdrawing groups improved the activity [24, 25]. Notably, the greatest activity was observed when 5-trifluoro-2-benzoic acid bonding to the sulfonamidyl linker was used (**5d**), leading to an enhanced antimicrobial activity with MICs of 2 and 4 μg/mL against *S. pneumoniae* and *S. aureus*, respectively.

Table 1. Antimicrobial activity of synthesized compounds **5a-5j**

Cpd.	R	MIC		
		SPNE	***SAUR[a]***	***SAUR[b]***
5a	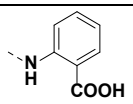	2	8	16
5b	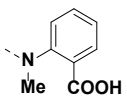	64	64	128
5c	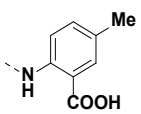	2	16	16

5d	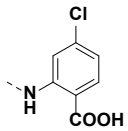	2	4	4
5e	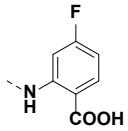	2	8	16
5f	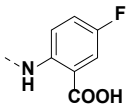	2	8	8
5g	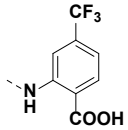	4	>256	>256
5h	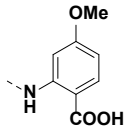	8	16	8
5i	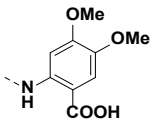	16	32	16
5j	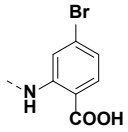	8	16	8
C3-005	\	8	16	16
Van	\	8+	2	2

SPNE: *S. pneumoniae* ATCC 49619, SAUR[a]: *S. aureus* ATCC 25923, SAUR[b]: *S. aureus* ATCC 29213.

Although **5b** showed reduced antimicrobial activity, we noticed that the substituents at the sulfonamidyl nitrogen may affect antimicrobial activity. Therefore, we generated **7a – 7k** and **10a – 10d** to thoroughly study the influence of substitutions on antimicrobial activity. Surprisingly, Table 2 shows that all these compounds demonstrated improved antimicrobial activity against some or all the tested bacterial strains. Notably, we observed that both aryl and aliphatic substituents were acceptable, demonstrating the potential for structural modifications on this site. Additionally, some compounds, such as **7a**, **7b**, **10a – 10d**, displayed superior antimicrobial activity against both *S. aureus* and *S. pneumoniae*, which was the first time being observed compared to other sigmacidin derivatives. Among the tested compounds, **7b** exhibited the highest activity against *S. aureus* with MIC values of 2 μg/mL. Interestingly, we noted that compounds with the same cyclopropylmethyl substituent on the sulfonamidyl nitrogen displayed varying levels of antimicrobial activity, in which the electron-donating groups on the right benzene ring (5-Me in **7a**) provided slightly more contribution to antimicrobial activity over the electron-withdrawing groups (4-F in **7f**, 4-Cl in **7i**, and 5-F in **7j**).

Table 2. Antimicrobial activity of synthesized compounds **7a-7k** and **10a-10d**

			MIC		
Cpd.	**R^2**	**R^1**			
			SPNE	***SAUR[a]***	***SAUR[b]***
7a	5-Me		2	4	4

7b	5-Me		4	2	2
7c	5-Me	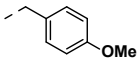	2	4	4
7d	5-Me	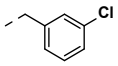	2	4	4
7e	5-Me	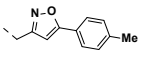	2	32	>256
7f	4-F		4	4	8
7g	4-F	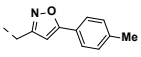	4	>256	16
7h	4-Cl	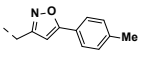	2	>256	>256
7i	4-Cl		4	4	4
7j	5-F		8	16	16
7k	5-F	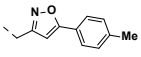	2p	>256	>256
10a	5-Me	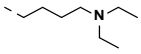	16	16	16
10b	5-Me	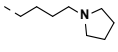	16	16	16
10c	5-Me	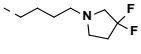	4	4	4
10d	5-Me	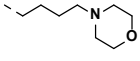	32	8	8

SPNE: *S. pneumoniae* ATCC 49619, SAUR[a]: *S. aureus* ATCC 25923, SAUR[b]: *S. aureus* ATCC 29213

With the preliminary antimicrobial activity of the compounds, we further screened the selected compounds against a panel of bacterial species from the WHO priority pathogens list [31] and clinically complex pathogens, including *Enterococcus faecalis* (EFAE), *Staphylococcus epidermidis* (SEPI), *Staphylococcus saprophyticus* (SSAP), *Streptococcus pyogenes* (SPYO), and *Streptococcus agalactiae* (SAGA), to validate the clinical prospect of our compounds.

The results depicted in Fig. 3 demonstrated the extensive antimicrobial potential of our compounds against a wide range of Gram-positive bacteria, including clinically complex pathogens, with most MICs ranging from 2 to 8 μg/mL. Notably, **5d**, **7a**, **7b** and **7d** presented robust antimicrobial activity against multiple Gram-positive bacteria, with an impressive MIC as low as 1 μg/mL against *S. pneumoniae*. Remarkably, **5d** exhibited significant potency against *Streptococci* (MIC 1-2 μg/mL), while **7a** demonstrated remarkable efficacy against *S. epidermidis* (MIC 2 μg/mL), showcasing the potential of our compounds in treating bacterial infections.

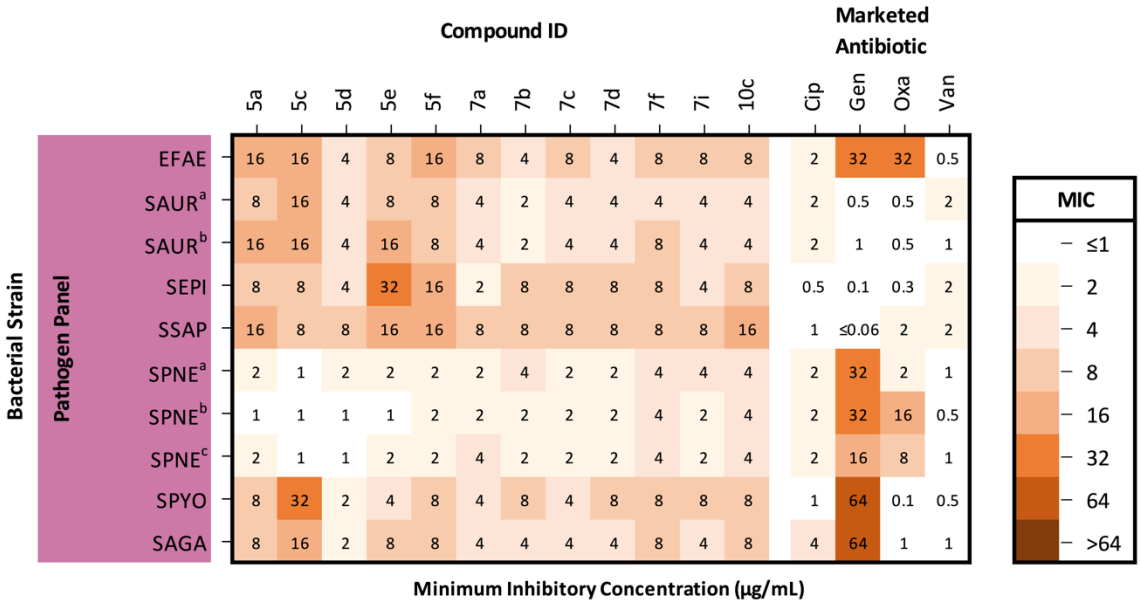

Fig. 3. Antimicrobial activity (MIC µg/mL) of the selected compounds against clinically important Gram-positive pathogens. Cip: Ciprofloxacin, Gen: Gentamicin, Oxa: Oxacillin, Van: Vancomycin.

Methicillin-resistant *S. aureus* (MRSA) strains represent some of the most challenging bacterial strains for treatment due to antibiotic resistance, including resistance to the "last resort" antimicrobial therapeutic agent, vancomycin, currently available in the market [33]. In order to evaluate the efficacy of our compounds against MRSA strains, we tested their activity against a series of representative clinically isolated lineages of hospital-acquired (HA-) and community-acquired (CA-) MRSA strains, including vancomycin-resistant *S. aureus* (VRSA) strains.

The HA-MRSA strains included W-231 ST45, W-232 ST5, W-233 ST5, W-234 ST-5, W-235 ST5, ATCC BAA-43, ATCC BAA-44, and ST239. The CA-MRSA strains, on the other hand, included W-45 ST59, W-46 ST59, W-47 ST30, W-48 ST217, ST22, ST338, and USA300. We also included several MRSA strains denoted as M20 [34]. To

further test our compounds, we included the laboratory strains of known resistant mechanisms, for example, SA-APH2”-AAC6’, SA-APH3’, and SA-ANT4’, which are resistant to aminoglycosides due to the presence of aminoglycoside-modifying enzymes (AMEs) [35]. We also included SA-RN4220-pUL5054, which exhibits macrolide resistance [36], as well as SA-1199B, which is known to be resistant to fluoroquinolone [37].

As shown in Fig. 4, our compounds demonstrated antimicrobial activity against the tested MRSA strains, with the most potent MIC as low as 2 μg/mL. This efficacy outperformed currently used antibiotics such as ciprofloxacin, gentamicin, and oxacillin, especially for treating specific strains. Notably, most of the MRSA strains selected were resistant to oxacillin, the current first-line antibiotic used in the U.S. for MRSA infections, as well as other common drugs like the protein-synthesis inhibitor gentamicin. Thus, the antimicrobial activity of our compounds against MRSA strains with various individual resistance mechanisms indicated diverse modes of action without overlapping with existing antibiotics. Among the compounds tested, **5d**, **7b**, **7c**, **7d**, and **7i** maintained consistent MIC values, ranging from 2 to 8 μg/mL, against a broad range of MRSA strains, particularly the aminoglycosides-resistant strain SA-APH3’, highlighting their potential for further development as treatments for MRSA infections.

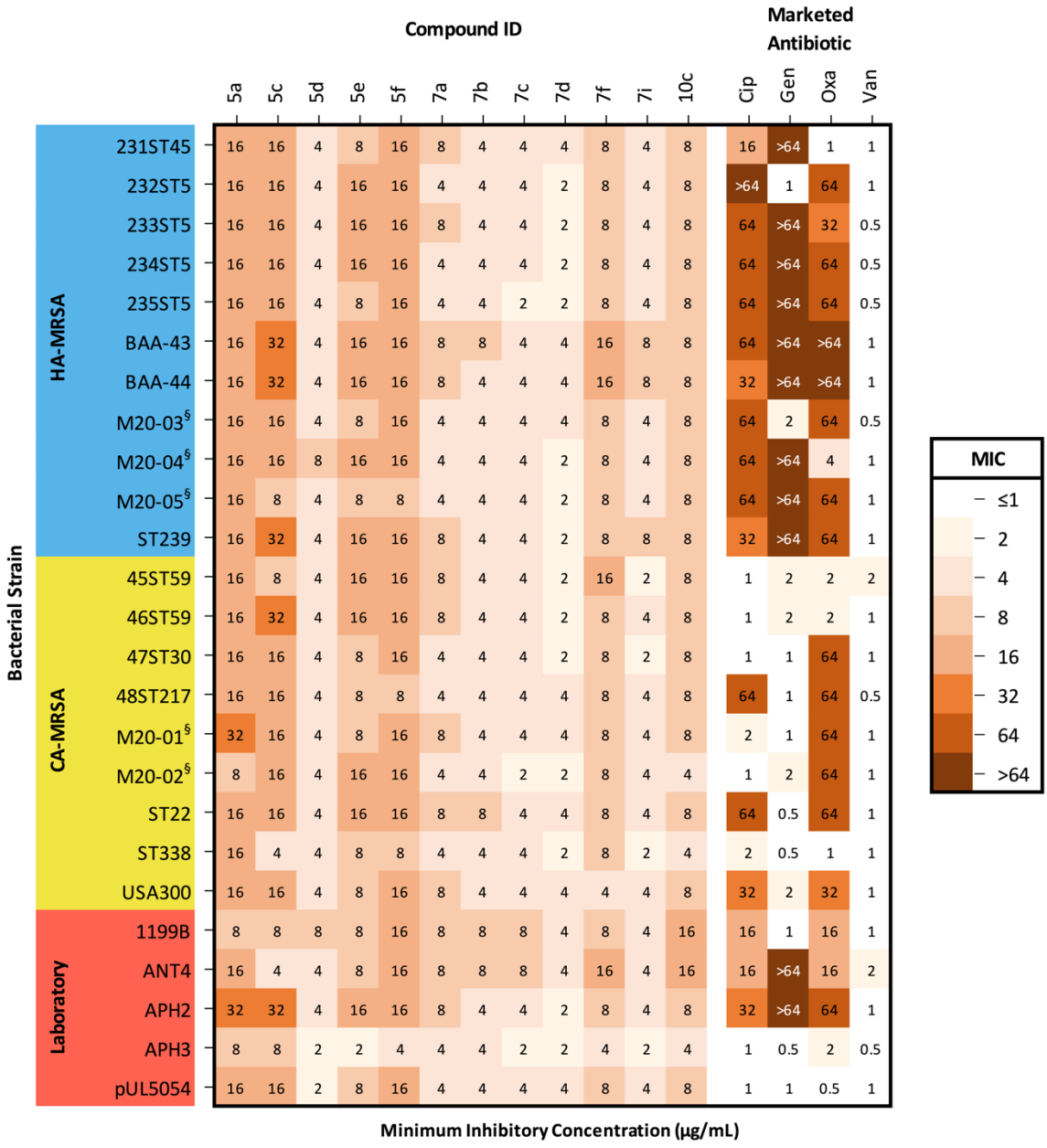

Fig. 4. Antimicrobial activity (MIC µg/mL) of the selected compounds against MRSA strains.

The VRSA strains used were provided by the Network on Antimicrobial Resistance in *S. aureus* (NARSA) for distribution by BEI Resources, NIAID, NIH and administered by ATCC (Manassas, Virginia, United States), which include: NR-46410 (*S. aureus* strain HIP11714), NR-46411 (*S. aureus* strain HIP11983), NR-46412 (*S. aureus* strain

HIP13170), NR-46413 (*S. aureus* strain HIP13419), NR-46414 (*S. aureus* strain HIP14300), NR-46415 (*S. aureus* strain HIP15178), NR-46416 (*S. aureus* strain AIS 2006032), NR-46417 (*S. aureus* strain AIS 2006045), NR-46418 (*S. aureus* strain 71080), NR- 46419 (*S. aureus* strain AIS 080003), NR-46420 (*S. aureus* strain AIS 1000505), NR-46421 (*S. aureus* strain AIS 1001095), and NR-46422 (*S. aureus* strain AID 1001123).

As shown in Fig. 5, several compounds exhibited remarkable antimicrobial activity against the tested VRSA strains with MIC as low as 2 μg/mL, whereas, in contrast, most strains were resistant towards or desensitised to cell wall synthesis inhibitors, vancomycin and oxacillin. The five compounds that effectively inhibit MRSA strains – **5d**, **7b**, **7c**, **7d**, and **7i** – consistently demonstrated antibacterial effects against VRSA strains, with MIC ranging from 2 to 8 μg/mL. Among these, **5d**, **7c** and **7d** demonstrated exceptionally superior antibacterial activity, with **5d** being highly effective in inhibiting strains NR-46418 and NR-46421 (MIC 2 μg/mL). Therefore, our compounds appeared effective against an array of VRSA strains harbouring multiple mechanisms of drug resistance, which strongly supports their clinical prospect and warrants further development as potential new treatment options against increasingly untenable and severe infections caused by VRSA.

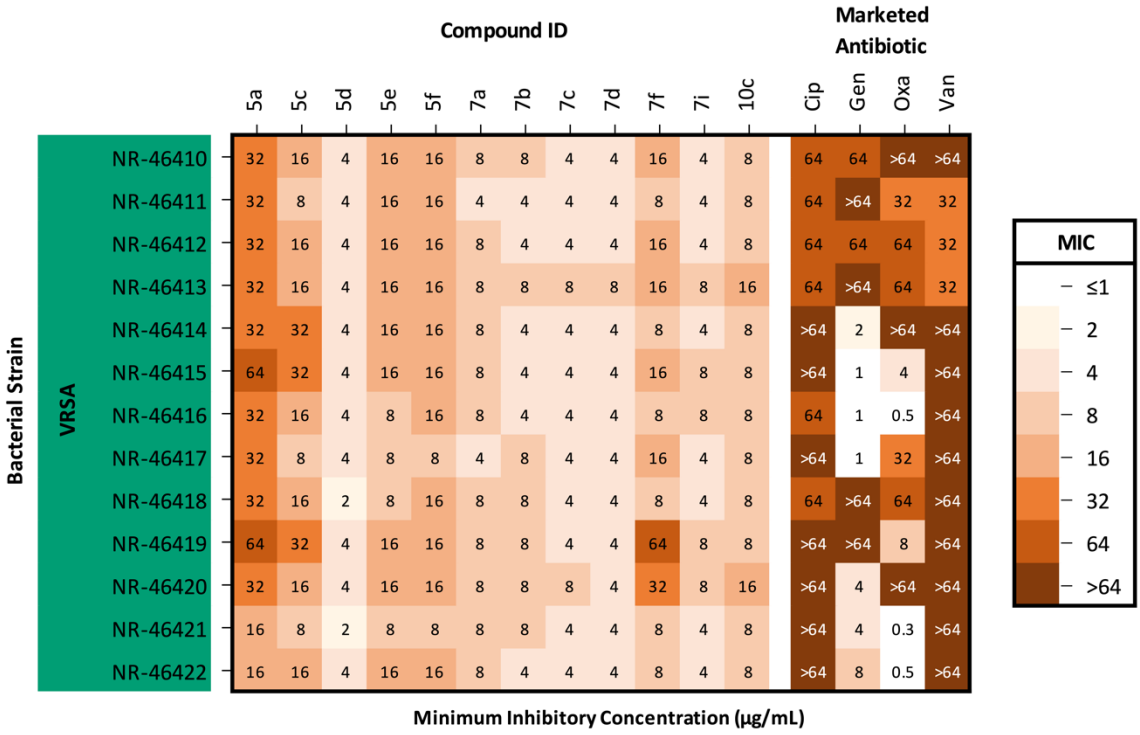

Fig. 5. Antimicrobial activity (MIC µg/mL) of the selected compounds against VRSA strains.

Taken together, the series of **C3** compounds exhibited significant antibacterial effects against a range of pathogenic bacteria, including notoriously difficult-to-treat strains such as MRSA and VRSA. The unsubstituted sulfonamidyl compounds (**5a – 5j**) maintained the strong antimicrobial activity against *S. pneumoniae* than other Gram-positive bacteria, while the substitutions at the sulfonamidyl nitrogen improved the general antimicrobial activity of the resulting compounds (**7a – 7k**) against *S. aureus*, as demonstrated by the testing results against MRSA and VRSA strains. Among the 12 compounds tested, **5d** and **7d** stood out with the highest antibacterial activity against a variety of bacterial strains that are resistant to currently available antibiotics.

2.4. β'CH - σ affinity inhibitory assay

As PPI inhibitors, the inhibitory activity of representative sulfonamidyl compounds was examined. Previously, we developed a luminescence-based protein complement assay [38], in which RNAP β'CH and σ are fused to the two complementary fragments of luciferase, respectively. Hence, when a PPI inhibitor targeting β'CH - σ interaction is used, the reformation of luciferase was hindered, leading to a decrease in luminescent signal. The results shown in Table 3 demonstrated that all the tested compounds showed inhibitory activity against β'CH - σ PPI.

Table 3. IC_{50} of selected compounds inhibiting β'CH – σ PPI.

	5d	**7a**	**7c**	**10c**
IC_{50} (μM)	121.35 ± 3.24	18.09 ± 0.61	62.88 ± 1.29	17.55 ± 0.37

It should be noted that the tested IC_{50} values did not correlate with the antimicrobial activity of the compounds. This phenomenon has been observed in previous studies, as the *in vivo* antimicrobial activity is significantly affected by multiple factors such as cell membrane permeability and efflux effects. Additionally, aqueous solubility of compounds may also affect the experimental process and so as IC_{50} values. Therefore, this assay should be used as a qualitative method to validate the molecular mechanism of compounds.

2.5. In vitro transcription assay

Inhibitory effects of compounds against RNAP activity were examined by a fluorescence-based *in vitro* transcription assay, in which the holoenzyme (core

saturated with σ^{70}) transcribed RNA malachite green aptamers for dye binding. Without any treatment, a significant fluorescence signal was detected compared to the rNTP-free control reaction (Fig. 6). A substantial decrease in fluorescence intensity was observed when compound **5d**/**7a**/**7c**/**10c** or rifampicin was added at 50 μM (Fig. 6). The result suggested that our compounds suppressed the *in vitro* processivity of RNAP.

Note that the inhibitory activity of compounds in the transcription assay may not strictly correlate to the data collected in the affinity assay. This is because transcription is a circulatory system, the σ factor needs to depart after the initiation of transcription occurred, which leaves the binding site at RNAP vacant and the inhibitors can occupy it before the next circle of transcription initiates. This specific biological mechanistic property renders PPI inhibitors particularly suitable for targeting transcription. Even though the binding affinity of PPI inhibitors are generally not as firm as enzyme inhibitors, the transcription circles provide PPI inhibitors more vigorous binding opportunities and lead to satisfying inhibitory effects.

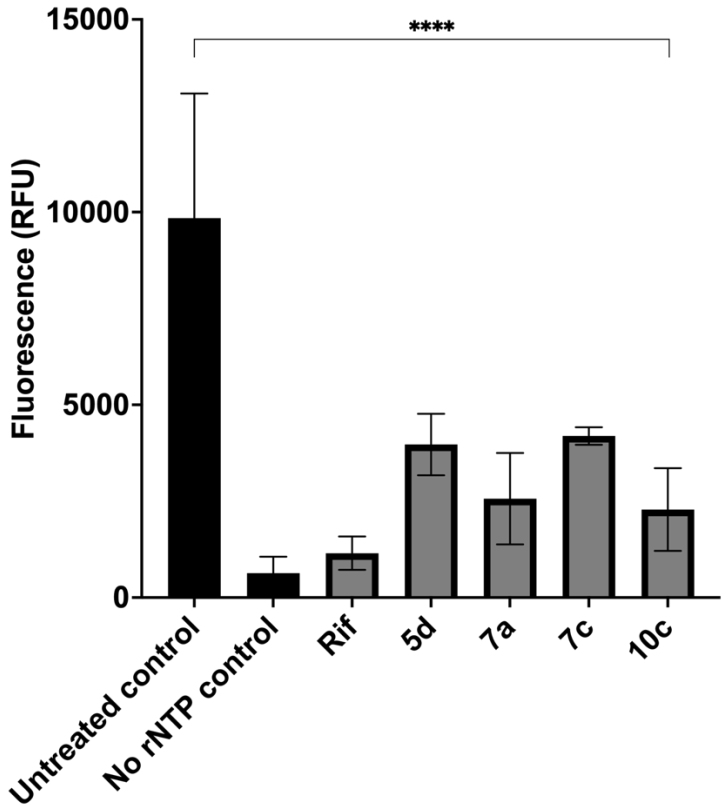

Fig. 6. *In vitro* transcription assay monitoring the RNAP activity under different treatments. Data were represented as means ± SEM. Technical repeats were performed for data reproducibility and a representative figure was shown. Rif: rifampicin. The data were represented in GraphPad Prism style. $p \leq 0.05$ (∗), ≤ 0.01 (∗∗), ≤ 0.001 (∗∗∗), ≤ 0.0001 (∗∗∗∗).

2.6. Confocal fluorescence microscope

Epifluorescence microscopy was employed to investigate the sub-cellular effects of compound **5d** on RNAP function. In this assay, the *B. subtilis* BS1048 strain, which the β' subunit was tagged by the green fluorescent protein (GFP) [39], was used to visualize RNAP localization. As shown in Fig. 6A, the GFP-labeled RNAP localized to the bacterial nucleoid. The administration of rifampicin, a RNAP-targeting antibiotic,

delocalized the transcription foci (Fig. 6B), while ribosome-targeting antibiotic chloramphenicol did not impact RNAP function (Fig. 6C). When compound **5d** was added, a concentration-dependent delocalization of the fluorescence signal from the nucleoid, similar to the effect observed in rifampicin-treated cells, was observed (Fig. 6D), suggesting that **5d** was an RNAP-σ PPI inhibitor that affected bacterial transcription as shown in the previous studies.

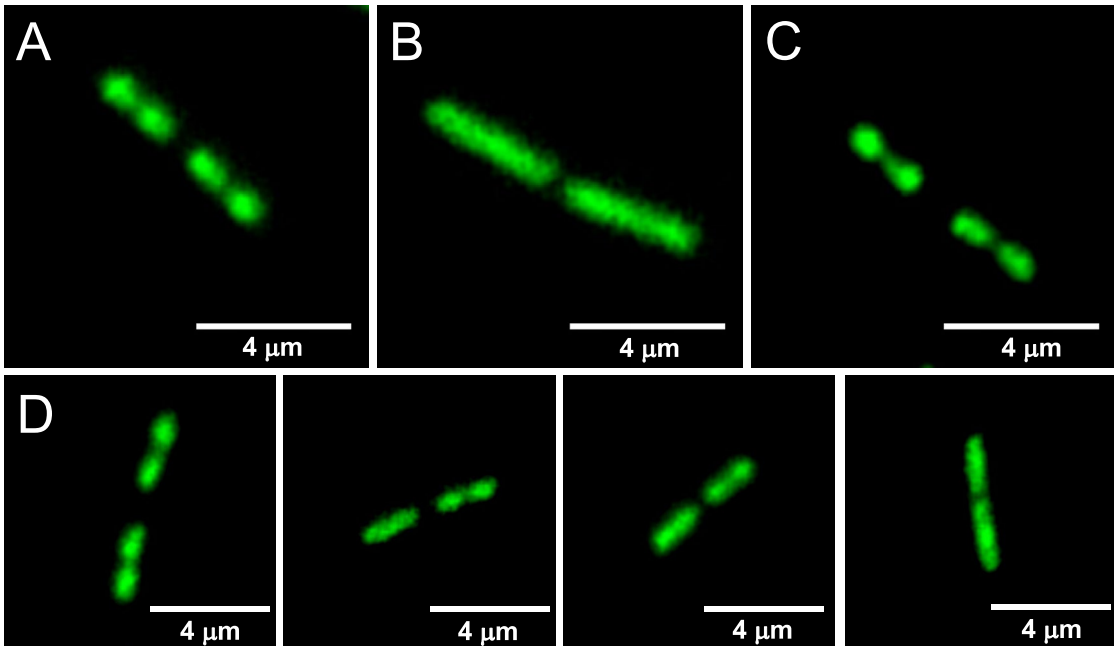

Fig. 7. **A**) Epifluorescence microscopic image of *B. subtilis* BS1048; **B**) *B. subtilis* BS1048 treated with rifampicin at 0.125 μg/mL; **C**) *B. subtilis* BS1048 treated with chloramphenicol at 4 μg/mL; **D**) *B. subtilis* BS1048 treated with **5d** (from left to right: 1, 2, 4, and 8 μg/mL).

2.7. Molecular docking

The PPI between β'CH and $\sigma_{2.2}$, including both the amino sequences and the secondary structures, are highly conserved across Gram-positive and Gram-negative bacteria [24-26]. Therefore, it is feasible to use β'CH from both classes of bacteria for molecular docking study. In the present research, β'CH extracted from the *E. coli* RNAP holoenzyme (PDB: 4LJZ) was used for docking studies, and the calculated binding poses of **5d** and **7d** in complex with β'CH were displayed in Fig. 8. As previously, the benzoic acid moieties of both ligands reside within the positive charged area formed by residues include R275 and R278, while the 3,4-dichlorophenyl ring fitted in a small pocket composed of hydrophobic residues. Additionally, the carboxyl group of **5d** established two hydrogen bonds with R278 (O…H 2.2 Å) and N274 (O…H 3.4 Å) within the β'CH region. Moreover, a hydrogen bond was formed between the nitro group and R275 (O…H 2.8 Å) (**Fig. 8B**). **Fig. 8C** showed the interactions between **7d** and β'CH, wherein the carboxyl group of **7d** interacted with R275 (O…H 2.1 Å) and R278 (O…H 2.2 Å) through hydrogen bonds, respectively. Meanwhile, R278 also interacted with the nitro group (O…H 2.9 Å). Overall, both compounds showed similar binding energies via the key interactions with the residues of β'CH including R275 and R278.

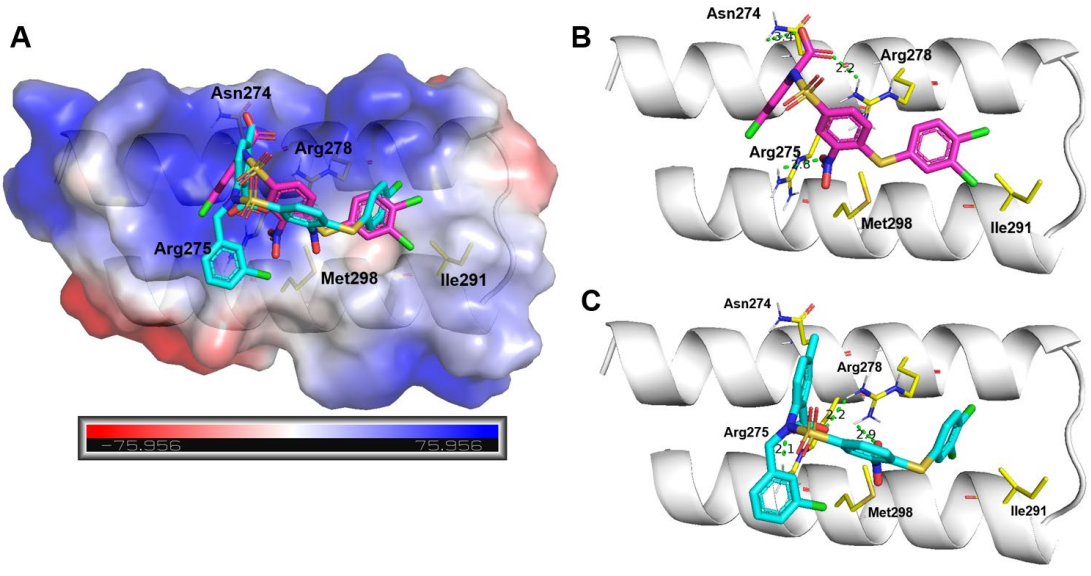

Fig. 8. The compounds were docked to β'CH using AutoDock Vina. (**A**) Binding poses of **5d** (magenta) and **7d** (cyan) in complex with β'CH. Details of the interactions between β'CH and **5d** (**B**) and **7d** (**C**). The images were generated by PyMol.

2.8. ADMET properties

To better understand the druggability of compounds **5d** and **7d**, we studied various ADMET (absorption, distribution, metabolism, excretion, and toxicity) parameters, such as water solubility (Ali log S), molar refractivity (MR), topological polar surface area (tPSA), Caco-2 cell permeability, intestinal absorption, the volume of distribution (VDss), unbound fraction of drug and ability to inhibit the P-glycoprotein substrate, using pkCSM [40].

Table 4 shows that both molecules are predicted to possess good water solubility and intestinal membrane permeability, as well as excellent human intestinal absorption, indicating drug-likeness and oral availability. Despite their relatively low volumes of distribution, as reflected by their MR and tPSA, and their low potential for binding to plasma proteins, the aforementioned properties, along with their potential for inhibiting P-glycoprotein, suggest that these compounds may be used for effective treatment of systemic infections with enhanced pharmacological activity.

Table 4. Predicted absorption and distribution properties of compounds **5d** and **7d**[a].

Ali log S[b]	MR[c]	tPSA ($Å^2$)[d]	Caco-2 permeability[e]	Human intestinal	VDss[g]	Fraction unbound[h]	P-gp inhibition[i]

					absorption (%)[f]			
5d	-9.51	124.93	162.97	0.64	77.37	-2.53	0	Yes
7d	-10.87	159.29	154.18	0.62	89.07	-2.35	0.174	Yes

[a] Parameters calculated using pkCSM [40]; [b] Aqueous solubility descriptor (≤ 0, log mol/L); [c] MR (molar refractivity) (≤ 155); [d] topological polar surface area (≤ 150 Å^2); [e] Caco-2 cell permeability (log Papp in 10^{-6} cm/s > 0.09); [f] absorption (human, % > 30); [g] volume of distribution (human, log L/kg) (low if < − 0.15 and high if > 0.45); [h] fraction unbound to plasma proteins; [i] ability to inhibit the P-glycoprotein

Given the promising calculated values, we then evaluated the cytotoxicity of selected compounds against human HepG2 hepatocellular carcinoma and A549 lung carcinoma cell lines. All the tested compounds demonstrated nearly no cytotoxicity to these two human cancer cell lines (Table 5), indicating our compounds have potential for further development.

Table 5. Cytotoxicity and therapeutic index of selected compounds

No.	MIC[a] (μg/mL)	CC_{50} (μM)		Therapeutic Index[b]	
		HepG2	A549	HepG2	A549
5c	2	3900 ± 3	24000 ± 3	1820	11200
5d	2	3410 ± 6	14800 ± 7	1710	7400
7d	2	387 ± 6	1840 ± 6	199	946
10c	4	145 ± 8	129 ± 7	145	129
DDP[c]	-	4.35 ± 0.2	5.26 ± 0.3	-	-

[a] MIC values against *S. pneumoniae* ATCC 49619.

[b] Calculated by CC_{50} / ½ MIC.

[c] DDP: Cisplatin

3. Conclusions

The discovery of PPI inhibitors is a challenging research field due to the relatively flat binding area of target proteins and their generally weak binding affinity. Previously, we have successfully developed indole derivatives as RNAP-σ PPI inhibitors [17, 41-45]. In this article, we explored the structural diversity of sulfonamidyl derivatives of **C3-005** (sigmacidins), and validated the antimicrobial activity, mechanism of action, cytotoxicity, and pharmacokinetic properties. The results indicated that the sulfonamidyl derivatives of **C3-005** were potential for further development. Specifically, the sulfonamidyl nitrogen provided an additional and appropriate position for substitution without diminishing antimicrobial activity. In contrast, the substituted derivatives demonstrated improved antimicrobial activity against *S. aureus*, including MRSA and VRSA. These results suggest that the development of structurally diverse derivatives of sigmacidin with excellent antimicrobial activity will expand the molecular pools of RNAP-σ PPI inhibitors for biomedical research and drug development. Additionally, it is worth mentioning that other PPIs in bacterial transcription, such as RNAP-NusA interaction, are essential for cell viability [46, 47], offering potential avenues for novel antibiotic drug design.

4. Experimental section

4.1. Chemistry

4.1.1. General methods

All reactions were monitored by thin-layer chromatography (TLC) on glass sheets (Silica gel F_{254}) which can be visualized under UV light. Flash chromatography was carried out using silica-gel (200 – 300 mesh). Commercial reagents and anhydrous solvents were used without further purification. All yields reported are isolated yields. ^{1}H NMR (400 MHz) and ^{13}C NMR (100 MHz) spectra were measured on BRUKER AVANCE-III spectrometer with TMS as an internal standard. Chemical shifts are expressed in δ (ppm) and coupling constants (*J*) in Hz. High resolution MS spectra were measured using a QTOF-2 micromass Spectrometer by electron spray ionization. HPLC analysis was performed on an Agilent 1260 HPLC apparatus.

4.1.2. General procedure for the synthesis of intermediates 3a – j (Scheme 1)

*General procedure for the synthesis of compound **3a** – **3o***

To a stirred solution of the anilines (1 mmol) in dichloromethane (DCM, 5 mL) at 0 °C was added pyridine (7.5 mmol). 4-Chloro-3-nitrobenzenesulfonyl chloride (1.2 mmol) in DCM (5 mL) was then added slowly via syringe. The solution was allowed to warm to room temperature and stirred for another 24 hrs. The mixture was diluted with DCM (10 ml) and washed by 1 M HCl and brine, successively. The organic phase was dried by Na_2SO_4 and purified by chromatography to provide the titled compounds.

*Methyl 2-((4-chloro-3-nitrophenyl)sulfonamido)benzoate (**3a**)*

Yellow solid (208 mg, 56 %). ^{1}H NMR (400 MHz, $CDCl_3$) δ 10.81 (s, 1H), 8.31 (d, *J* = 2.0 Hz, 1H), 7.95 (ddd, *J* = 10.9, 8.2, 1.6 Hz, 2H), 7.71 (d, *J* = 8.3 Hz, 1H), 7.62 (d, *J* = 8.5 Hz, 1H), 7.57 – 7.51 (m, 1H), 7.14 (t, *J* = 7.6 Hz, 1H), 3.90 (s, 3H).

*Methyl 2-((4-chloro-N-methyl-3-nitrophenyl)sulfonamido)benzoate (**3b**)*

White solid (227 mg, 59 %). ^{1}H NMR (400 MHz, $CDCl_3$) δ 8.12 (d, *J* = 2.0 Hz, 1H), 7.91 (dd, *J* = 7.7, 1.6 Hz, 1H), 7.77 (dd, *J* = 8.4, 2.0 Hz, 1H), 7.66 (d, *J* = 8.4 Hz, 1H), 7.52 (td, *J* = 7.7, 1.6 Hz, 1H), 7.46 (td, *J* = 7.4, 0.9 Hz, 1H), 7.10 (dd, *J* = 7.8, 0.7 Hz, 1H), 3.81 (s, 3H), 3.34 (s, 3H).

*Methyl 2-((4-chloro-3-nitrophenyl)sulfonamido)-5-methylbenzoate (**3c**)*

Red solid (196 mg, 51 %). ^{1}H NMR (400 MHz, $CDCl_3$) δ 10.55 (s, 1H), 8.27 (d, *J* = 1.9 Hz, 1H), 7.90 (dd, *J* = 8.4, 2.0 Hz, 1H), 7.75 (s, 1H), 7.61 (dd, *J* = 8.3, 6.4 Hz, 2H), 7.34 (dd, *J* = 8.4, 1.2 Hz, 1H), 3.88 (s, 3H).

*Methyl 4-chloro-2-((4-chloro-3-nitrophenyl)sulfonamido)benzoate (**3d**)*

White solid (223 mg, 55 %). ^{1}H NMR (400 MHz, $CDCl_3$) δ 10.94 (s, 1H), 8.36 (d, *J* = 2.0 Hz, 1H), 8.00 (dd, *J* = 8.4, 2.0 Hz, 1H), 7.93 (d, *J* = 8.6 Hz, 1H), 7.77 F(d, *J* = 1.8 Hz, 1H), 7.69 (d, *J* = 8.4 Hz, 1H), 7.13 (dd, *J* = 8.5, 1.8 Hz, 1H), 3.94 (s, 3H).

*Methyl 2-((4-chloro-3-nitrophenyl)sulfonamido)-4-fluorobenzoate (**3e**)*

White solid (202 mg, 52 %). ^{1}H NMR (400 MHz, $CDCl_3$) δ 11.08 (s, 1H), 8.34 (d, *J* = 1.9 Hz, 1H), 8.04 – 7.95 (m, 2H), 7.67 (d, *J* = 8.5 Hz, 1H), 7.46 (dd, *J* = 10.4, 2.3 Hz, 1H), 6.87 – 6.76 (m, 1H), 3.92 (s, 3H).

*Methyl 5-fluoro-2-((4-fluoro-3-nitrophenyl)sulfonamido)benzoate (**3f**)*

Brown solid (208 mg, 56 %); ^{1}H NMR (400 MHz, $CDCl_3$) δ 10.44 (s, 1H), 8.26 (d, *J* = 2.1 Hz, 1H), 7.88 (dd, *J* = 8.5, 2.1 Hz, 1H), 7.74 (dd, *J* = 9.1, 4.7 Hz, 1H), 7.67 – 7.58 (m, 2H), 7.30 – 7.24 (m, 1H).

*Methyl 2-((4-chloro-3-nitrophenyl)sulfonamido)-4-(trifluoromethyl)benzoate (**3g**)*

Yellow solid (272 mg, 62 %). ^{1}H NMR (400 MHz, $CDCl_3$) δ 10.93 (s, 1H), 8.36 (d, *J* = 2.0 Hz, 1H), 8.13 (d, *J* = 8.2 Hz, 1H), 8.03 (s, 1H), 7.99 (dd, *J* = 8.5, 2.1 Hz, 1H), 7.69 (d, *J* = 8.4 Hz, 1H), 7.40 (d, *J* = 8.2 Hz, 1H), 3.98 (s, 3H).

*Methyl 2-((4-chloro-3-nitrophenyl)sulfonamido)-4-methoxybenzoate (**3h**)*

White solid (200 mg, 50 %). ^{1}H NMR (400 MHz, $CDCl_3$) δ 11.04 (s, 1H), 8.34 (d, *J* = 2.1 Hz, 1H), 7.96 (dd, *J* = 8.5, 2.1 Hz, 1H), 7.89 (d, *J* = 8.9 Hz, 1H), 7.64 (d, *J* = 8.5 Hz, 1H), 7.22 (d, *J* = 2.4 Hz, 1H), 6.62 (dd, *J* = 8.9, 2.4 Hz, 1H), 3.87 (s, 3H), 3.86 (s, 3H).

*Methyl 2-((4-chloro-3-nitrophenyl)sulfonamido)-4,5-dimethoxybenzoate (**3i**)*

Red solid (250 mg, 58 %). ^{1}H NMR (400 MHz, $CDCl_3$) δ 10.56 (s, 1H), 8.26 (d, *J* = 2.1 Hz, 1H), 7.85 (dd, *J* = 8.5, 2.1 Hz, 1H), 7.60 (d, *J* = 8.5 Hz, 1H), 7.31 (d, *J* = 11.0 Hz, 2H), 3.97 (s, 3H), 3.85 (s, 6H).

*Methyl 4-bromo-2-((4-chloro-3-nitrophenyl)sulfonamido)benzoate (**3j**)*

White solid (297 mg, 66 %). ^{1}H NMR (400 MHz, $CDCl_3$) δ 10.88 (s, 1H), 8.34 (d, *J* = 2.0 Hz, 1H), 7.97 (dd, *J* = 8.5, 2.1 Hz, 1H), 7.91 (d, *J* = 1.5 Hz, 1H), 7.82 (d, *J* = 8.6 Hz, 1H), 7.67 (d, *J* = 8.4 Hz, 1H), 7.28 (d, *J* = 1.8 Hz, 1H), 3.91 (s, 3H).

*Methyl 1-((4-chloro-3-nitrophenyl)sulfonamido)cyclopropane-1-carboxylate (**3k**)*

Yellow solid (241 mg, 72 %). ^{1}H NMR (400 MHz, $CDCl_3$) δ 8.33 (d, *J* = 2.0 Hz, 1H), 8.00 (dd, *J* = 8.4, 2.0 Hz, 1H), 7.72 (d, *J* = 8.4 Hz, 1H), 5.62 (s, 1H), 3.45 (s, 3H), 1.54 (t, *J* = 2.7 Hz, 2H), 1.51 (d, *J* = 3.3 Hz, 2H).

*Methyl ((4-chloro-3-nitrophenyl)sulfonyl)-L-valinate (**3l**)*

White solid (263 mg, 75 %). ^{1}H NMR (400 MHz, $CDCl_3$) δ 8.31 (d, *J* = 2.1 Hz, 1H), 7.98 (dd, *J* = 8.5, 2.1 Hz, 1H), 7.73 (d, *J* = 8.5 Hz, 1H), 5.23 (d, *J* = 9.8 Hz, 1H), 3.86 (dd, *J* = 10.0, 4.9 Hz, 1H), 2.14 (qd, *J* = 12.1, 6.8 Hz, 1H), 1.02 (d, *J* = 6.8 Hz, 3H), 0.91 (d, *J* = 6.9 Hz, 3H).

*Methyl ((4-chloro-3-nitrophenyl)sulfonyl)-L-phenylalaninate (**3m**)*

White solid (275 mg, 69 %). ^{1}H NMR (400 MHz, $CDCl_3$) δ 8.12 (d, *J* = 2.0 Hz, 1H), 7.77 (dd, *J* = 8.4, 2.1 Hz, 1H), 7.58 (d, *J* = 8.5 Hz, 1H), 7.27 – 7.17 (m, 3H), 7.06 (dd, *J* = 6.2, 2.9 Hz, 2H), 5.25 (d, *J* = 9.4 Hz, 1H), 4.29 (ddd, *J* = 9.3, 7.8, 5.1 Hz, 1H), 3.70 (s, 3H), 3.15 (dd, *J* = 13.9, 5.0 Hz, 1H), 2.97 (dd, *J* = 13.9, 7.7 Hz, 1H).

*Methyl ((4-chloro-3-nitrophenyl)sulfonyl)-L-alaninate (**3n**)*

White solid (229 mg, 71 %). ^{1}H NMR (400 MHz, $CDCl_3$) δ 8.32 (d, *J* = 2.1 Hz, 1H), 7.98 (dd, *J* = 8.4, 2.1 Hz, 1H), 7.72 (d, *J* = 8.5 Hz, 1H), 5.39 (d, *J* = 8.2 Hz, 1H), 4.16 – 4.03 (m, 1H), 3.64 (s, 3H), 1.45 (d, *J* = 7.2 Hz, 3H).

*4-Chloro-N-(2-(hydroxymethyl)phenyl)-3-nitrobenzenesulfonamide (**3o**)*

Pale yellow solid (257 mg, 75 %). ^{1}H NMR (400 MHz, $CDCl_3$) δ 8.27 (d, *J* = 2.0 Hz, 1H), 8.24 (s, 1H), 7.89 (dd, *J* = 8.4, 2.1 Hz, 1H), 7.63 (d, *J* = 8.4 Hz, 1H), 7.51 (d, *J* = 8.1 Hz, 1H), 7.31 (d, *J* = 8.1 Hz, 1H), 7.14 (q, *J* = 7.2 Hz, 2H), 4.49 (d, *J* = 4.6 Hz, 2H), 2.09 – 2.01 (m, 1H).

*General procedure for the synthesis of compound **4a** – **4o***

To a flask was added compound **3a** – **3o** (0.3 mmol), 3,4-dichlorobenzenethiol (0.5 mmol), NaOAc (1.5 mmol) and ethanol (EtOH, 3 ml), the mixture was heated to reflux for 6 hrs and then cooled to room temperature. The precipitate was collected by filtration and washed by a small amount of EtOH and water, successively. The filter cake was dried in vacuum to afford compound **4a** – **4o**.

*Methyl 2-((4-((3,4-dichlorophenyl)thio)-3-nitrophenyl)sulfonamido)benzoate (**4a**)*

Yellow solid (116 mg, 75 %); ^{1}H NMR (400 MHz, $CDCl_3$) δ 10.82 (s, 1H), 8.69 (d, *J* = 2.0 Hz, 1H), 7.96 (dd, *J* = 7.9, 1.2 Hz, 1H), 7.79 (dd, *J* = 8.7, 1.9 Hz, 1H), 7.69 (d, *J* = 8.3 Hz, 1H), 7.65 (d, *J* = 1.9 Hz, 1H), 7.59 (d, *J* = 8.3 Hz, 1H), 7.54 – 7.46 (m, 1H),

7.38 (dd, *J* = 8.2, 2.0 Hz, 1H), 7.10 (t, *J* = 7.6 Hz, 1H), 6.90 (d, *J* = 8.7 Hz, 1H), 3.90 (s, 3H).

*Methyl 2-((4-((3,4-dichlorophenyl)thio)-N-methyl-3-nitrophenyl)sulfonamido)benzoate (**4b**)*

Yellow solid (100 mg, 63 %); ^{1}H NMR (400 MHz, $CDCl_3$) δ 8.51 (d, *J* = 1.9 Hz, 1H), 7.89 (dd, *J* = 7.6, 1.6 Hz, 1H), 7.71 (d, *J* = 1.9 Hz, 1H), 7.63 – 7.58 (m, 2H), 7.49 (td, *J* = 7.7, 1.7 Hz, 1H), 7.46 – 7.40 (m, 2H), 7.08 (d, *J* = 7.6 Hz, 1H), 6.94 (d, *J* = 8.6 Hz, 1H), 3.82 (s, 3H), 3.30 (s, 3H).

*Methyl 2-((4-((3,4-dichlorophenyl)thio)-3-nitrophenyl)sulfonamido)-5-methylbenzoate (**4c**)*

Yellow solid (125 mg, 79 %); ^{1}H NMR (400 MHz, $CDCl_3$) δ 10.57 (s, 1H), 8.65 (d, *J* = 1.9 Hz, 1H), 7.75 (dd, *J* = 8.7, 1.9 Hz, 2H), 7.65 (d, *J* = 1.9 Hz, 1H), 7.60 (dd, *J* = 8.3, 5.5 Hz, 2H), 7.38 (dd, *J* = 8.2, 2.0 Hz, 1H), 7.31 (dd, *J* = 8.4, 1.5 Hz, 1H), 6.88 (d, *J* = 8.6 Hz, 1H), 3.87 (s, 3H), 2.29 (s, 3H).

*Methyl 4-chloro-2-((4-((3,4-dichlorophenyl)thio)-3-nitrophenyl)sulfonamido)benzoate (**4d**)*

Yellow solid (141 mg, 86 %); ^{1}H NMR (400 MHz, $CDCl_3$) δ 10.92 (s, 1H), 8.72 (d, *J* = 2.0 Hz, 1H), 7.90 (dd, *J* = 8.5, 3.6 Hz, 1H), 7.81 (dd, *J* = 8.6, 2.0 Hz, 1H), 7.70 (dd, *J* = 21.8, 1.9 Hz, 2H), 7.60 (d, *J* = 8.2 Hz, 1H), 7.39 (dd, *J* = 8.3, 2.0 Hz, 1H), 7.07 (dd, *J* = 8.6, 1.8 Hz, 1H), 6.94 (d, *J* = 8.6 Hz, 1H), 3.91 (s, 3H).

Methyl 2-((4-((3,4-dichlorophenyl)thio)-3-nitrophenyl)sulfonamido)-4-fluorobenzoate ***(4e)***

Yellow solid (123 mg, 77 %). ^{1}H NMR (400 MHz, $CDCl_3$) δ 11.08 (s, 1H), 8.73 (d, *J* = 1.8 Hz, 1H), 8.00 (dd, *J* = 8.9, 6.3 Hz, 1H), 7.82 (dd, *J* = 8.7, 1.8 Hz, 1H), 7.67 (d, *J* = 1.7 Hz, 1H), 7.60 (d, *J* = 8.3 Hz, 1H), 7.41 (ddd, *J* = 10.1, 9.5, 2.1 Hz, 2H), 6.93 (d, *J* = 8.7 Hz, 1H), 6.78 (td, *J* = 9.0, 2.3 Hz, 1H), 3.91 (s, 3H).

Methyl 2-((4-((3,4-dichlorophenyl)thio)-3-nitrophenyl)sulfonamido)-5-fluorobenzoate ***(4f)***

Yellow solid (128 mg, 80 %). ^{1}H NMR (400 MHz, $CDCl_3$) δ 10.49 (s, 1H), 8.65 (d, *J* = 1.8 Hz, 1H), 7.77 – 7.70 (m, 2H), 7.63 (ddd, *J* = 14.4, 8.3, 5.1 Hz, 3H), 7.39 (dd, *J* = 8.3, 1.9 Hz, 1H), 7.25 – 7.21 (m, 1H), 6.90 (d, *J* = 8.7 Hz, 1H), 3.90 (s, 3H).

*Methyl 2-((4-((3,4-dichlorophenyl)thio)-3-nitrophenyl)sulfonamido)-4-(trifluoromethyl)benzoate (****4g****)*

Yellow solid (141 mg, 81 %); ^{1}H NMR (400 MHz, $CDCl_3$) δ 10.96 (s, 1H), 8.71 (d, *J* = 1.9 Hz, 1H), 8.10 (d, *J* = 8.3 Hz, 1H), 7.98 (s, 1H), 7.81 (dd, *J* = 8.7, 1.9 Hz, 1H), 7.65 (d, *J* = 1.8 Hz, 1H), 7.60 (d, *J* = 8.2 Hz, 1H), 7.43 – 7.36 (m, 2H), 7.33 (d, *J* = 8.3 Hz, 1H), 6.94 (d, *J* = 8.7 Hz, 1H), 3.95 (s, 1H).

*Methyl 2-((4-((3,4-dichlorophenyl)thio)-3-nitrophenyl)sulfonamido)-4-methoxybenzoate (****4h****)*

Yellow solid (139 mg, 85 %). ^{1}H NMR (400 MHz, $CDCl_3$) δ 11.05 (s, 1H), 8.73 (d, *J* = 1.9 Hz, 1H), 7.88 (d, *J* = 8.9 Hz, 1H), 7.79 (dd, *J* = 8.7, 2.0 Hz, 1H), 7.66 (d, *J* = 2.0 Hz, 1H), 7.60 (d, *J* = 8.3 Hz, 1H), 7.39 (dd, *J* = 8.2, 2.0 Hz, 1H), 7.23 (d, *J* = 2.4 Hz, 1H), 6.91 (d, *J* = 8.7 Hz, 1H), 6.59 (dd, *J* = 8.9, 2.4 Hz, 1H), 3.86 (s, 3H), 3.85 (s, 3H).

*Methyl 2-((4-((3,4-dichlorophenyl)thio)-3-nitrophenyl)sulfonamido)-4,5-dimethoxybenzoate (**4i**)*

Yellow solid (151 mg, 88 %); ^{1}H NMR (400 MHz, $CDCl_3$) δ 10.62 (s, 1H), 8.65 (d, *J* = 1.9 Hz, 1H), 7.71 (dd, *J* = 8.6, 1.9 Hz, 1H), 7.66 (d, *J* = 1.9 Hz, 1H), 7.60 (d, *J* = 8.3 Hz, 1H), 7.38 (dd, *J* = 8.2, 1.9 Hz, 1H), 7.32 (d, *J* = 1.4 Hz, 2H), 6.87 (d, *J* = 8.7 Hz, 1H), 3.96 (s, 3H), 3.85 (s, 3H), 3.84 (s, 3H).

*Methyl 4-bromo-2-((4-((3,4-dichlorophenyl)thio)-3-nitrophenyl)sulfonamido)benzoate (**4j**)*

White solid (170 mg, 96 %); ^{1}H NMR (400 MHz, $CDCl_3$) δ 10.88 (s, 1H), 8.72 (d, *J* = 2.0 Hz, 1H), 7.89 (d, *J* = 1.7 Hz, 1H), 7.84 – 7.77 (m, 2H), 7.67 (d, *J* = 1.9 Hz, 1H), 7.59 (s, 1H), 7.40 (dd, *J* = 8.3, 2.0 Hz, 1H), 7.23 (dd, *J* = 8.6, 1.7 Hz, 1H), 6.94 (d, *J* = 8.6 Hz, 1H), 3.91 (s, 3H).

*Methyl 1-((4-((3,4-dichlorophenyl)thio)-3-nitrophenyl)sulfonamido)cyclopropane-1-carboxylate (**4k**)*

Yellow solid (113 mg, 79 %); ^{1}H NMR (400 MHz, $CDCl_3$) δ 8.71 (d, *J* = 1.9 Hz, 1H), 7.82 (dd, *J* = 8.6, 1.9 Hz, 1H), 7.70 (d, *J* = 1.9 Hz, 1H), 7.62 (d, *J* = 8.3 Hz, 1H), 7.42

(dd, *J* = 8.3, 2.0 Hz, 1H), 6.98 (d, *J* = 8.6 Hz, 1H), 3.45 (s, 3H), 1.49 (q, *J* = 3.1 Hz, 4H).

*Methyl ((4-((3,4-dichlorophenyl)thio)-3-nitrophenyl)sulfonyl)-L-valinate (**4l**)*

Yellow solid (113 mg, 79 %); ^{1}H NMR (400 MHz, $CDCl_3$) δ 8.66 (d, *J* = 1.9 Hz, 1H), 7.77 (dd, *J* = 8.7, 2.0 Hz, 1H), 7.69 (d, *J* = 1.9 Hz, 1H), 7.62 (d, *J* = 8.3 Hz, 1H), 7.42 (dd, *J* = 8.3, 2.0 Hz, 1H), 6.97 (d, *J* = 8.7 Hz, 1H), 5.19 (d, *J* = 8.7 Hz, 1H), 3.83 (dd, *J* = 8.6, 4.7 Hz, 1H), 3.55 (s, 3H), 2.09 (qt, *J* = 12.8, 6.5 Hz, 1H), 0.98 (d, *J* = 6.8 Hz, 3H), 0.88 (d, *J* = 6.9 Hz, 3H).

*Methyl ((4-((3,4-dichlorophenyl)thio)-3-nitrophenyl)sulfonyl)-L-phenylalaninate (**4m**)*

Yellow solid (135 mg, 83 %); ^{1}H NMR (400 MHz, $CDCl_3$) δ 8.47 (d, *J* = 1.9 Hz, 1H), 7.69 (d, *J* = 2.0 Hz, 1H), 7.64 – 7.57 (m, 2H), 7.42 (dd, *J* = 8.3, 2.0 Hz, 1H), 7.19 (dd, *J* = 4.9, 1.5 Hz, 3H), 7.03 (dd, *J* = 6.5, 2.7 Hz, 2H), 6.84 (d, *J* = 8.7 Hz, 1H), 5.19 (s, 1H), 4.23 (s, 1H), 3.66 (s, 3H), 3.10 (dd, *J* = 13.9, 5.1 Hz, 1H), 2.94 (dd, *J* = 13.9, 7.5 Hz, 1H).

*Methyl ((4-((3,4-dichlorophenyl)thio)-3-nitrophenyl)sulfonyl)-L-alaninate (**4n**)*

Yellow solid (107 mg, 77 %); ^{1}H NMR (400 MHz, $CDCl_3$) δ 8.71 (d, *J* = 2.0 Hz, 1H), 7.81 (dd, *J* = 8.6, 2.0 Hz, 1H), 7.72 (d, *J* = 2.0 Hz, 1H), 7.64 (d, *J* = 8.2 Hz, 1H), 7.45 (dd, *J* = 8.3, 2.0 Hz, 1H), 7.00 (d, *J* = 8.6 Hz, 1H), 5.32 (d, *J* = 2.7 Hz, 1H), 4.09 (dd, *J* = 13.9, 6.9 Hz, 1H), 3.66 (s, 3H), 1.46 (d, *J* = 7.1 Hz, 3H).

*4-((3,4-Dichlorophenyl)thio)-N-(2-(hydroxymethyl)phenyl)-3-nitrobenzenesulfonamide (**4o**)*

Yellow solid (123 mg, 85 %). mp 156 – 158 ℃. ^{1}H NMR (400 MHz, DMSO-d_6) δ 9.84 (s, 1H), 8.44 (d, J = 1.7 Hz, 1H), 8.01 (d, J = 1.6 Hz, 1H), 7.85 (d, J = 8.3 Hz, 1H), 7.77 (dd, J = 8.6, 1.8 Hz, 1H), 7.65 (dd, J = 8.3, 1.8 Hz, 1H), 7.44 (d, J = 7.4 Hz, 1H), 7.23 (t, J = 7.3 Hz, 1H), 7.19 – 7.11 (m, 2H), 6.89 (d, J = 7.8 Hz, 1H), 5.18 (s, 1H), 4.44 (s, 2H). ^{13}C NMR (100 MHz, DMSO-d_6) δ 144.6, 142.9, 139.1, 138.2, 137.3, 136.0, 134.4, 133.3, 133.1, 132.9, 131.9, 130.7, 130.2, 128.1, 127.7, 127.2, 126.1, 124.6, 59.6. HRMS (ESI): calcd for $C_{19}H_{13}Cl_2N_2O_5S_2$, $[M-H]^-$ 482.9648, found 482.9647. HPLC purity: 98.68 %.

*General procedure for the synthesis of compound **5a** – **5n**.*

The methyl esters of compounds (**4a** – **4n**) (0.1 mmol) were hydrolyzed with 1 M NaOH in dioxane (1 : 1) at 50 ℃ overnight. The mixture was then diluted with a small amount of water and washed twice by DCM. The aqueous solution was acidified by the addition of 2 M HCl. The precipitates were collected by filtration and washed with water to provide the title compounds **5a** – **5n**.

*2-((4-((3,4-Dichlorophenyl)thio)-3-nitrophenyl)sulfonamido)benzoic acid (**5a**)*

Yellow solid (26 mg, 53 %). mp 243 – 245 ℃. ^{1}H NMR (400 MHz, DMSO-d_6) δ 11.57 (s, 1H), 8.55 (s, 1H), 7.99 (s, 1H), 7.90 (d, J = 8.2 Hz, 2H), 7.84 (d, J = 8.3 Hz, 1H), 7.63 (d, J = 8.1 Hz, 1H), 7.54 (t, J = 7.5 Hz, 1H), 7.46 (d, J = 8.1 Hz, 1H), 7.16 (t, J = 7.4 Hz, 1H), 7.10 (d, J = 8.6 Hz, 1H). ^{13}C NMR (100 MHz, DMSO-d_6) δ 169.8, 144.6, 143.5, 139.6, 137.4, 137.1, 136.1, 134.8, 134.6, 133.3, 133.0, 132.0, 131.9, 130.4, 130.2,

124.9, 124.3, 119.9, 118.8. HRMS (ESI): calcd for $C_{19}H_{11}Cl_2N_2O_6S_2$, $[M-H]^-$ 496.9441, found 496.9455. HPLC purity: 98.05 %.

2-((4-((3,4-Dichlorophenyl)thio)-N-methyl-3-nitrophenyl)sulfonamido)benzoic acid ***(5b)***

Yellow solid (23 mg, 45 %). mp 198 – 200 °C. ^{1}H NMR (400 MHz, DMSO-d_6) δ 12.81 (s, 1H), 8.27 (s, 1H), 8.03 (s, 1H), 7.87 (d, J = 8.3 Hz, 1H), 7.78 (d, J = 7.0 Hz, 1H), 7.69 (t, J = 8.1 Hz, 2H), 7.55 – 7.44 (m, 2H), 7.16 (d, J = 8.6 Hz, 1H), 7.08 (d, J = 7.4 Hz, 1H), 3.21 (s, 3H). ^{13}C NMR (100 MHz, DMSO-d_6) δ 167.5, 144.7, 142.9, 139.3, 137.3, 136.2, 136.0, 134.5, 133.4, 133.3, 133.0, 132.8, 132.4, 131.1, 130.7, 130.1, 129.6, 129.1, 125.0, 39.4. HRMS (ESI): calcd for $C_{20}H_{13}Cl_2N_2O_6S_2$, $[M-H]^-$ 510.9598, found 510.9595. HPLC purity: 97.12 %.

2-((4-((3,4-Dichlorophenyl)thio)-3-nitrophenyl)sulfonamido)-5-methylbenzoic acid ***(5c)***

Yellow solid (31 mg, 60 %). mp 128 – 130 °C. ^{1}H NMR (400 MHz, DMSO-d_6) δ 11.35 (s, 1H), 8.51 (d, J = 1.9 Hz, 1H), 7.98 (d, J = 1.6 Hz, 1H), 7.84 (dd, J = 8.5, 2.7 Hz, 2H), 7.69 (s, 1H), 7.62 (dd, J = 8.3, 1.8 Hz, 1H), 7.36 (s, 2H), 7.08 (d, J = 8.7 Hz, 1H), 2.24 (s, 3H). ^{13}C NMR (100 MHz, DMSO-d_6) δ 169.7, 144.5, 143.4, 137.4, 137.1, 136.8, 136.1, 135.3, 134.6, 133.8, 133.3, 133.0, 132.0, 131.9, 130.4, 130.2, 124.8, 120.5, 119.2, 20.5. HRMS (ESI): calcd for $C_{20}H_{13}Cl_2N_2O_6S_2$, $[M-H]^-$ 510.9598, found 510.9607. HPLC purity: 99.67 %.

4-Chloro-2-((4-((3,4-dichlorophenyl)thio)-3-nitrophenyl)sulfonamido)benzoic acid ***(5d)***

Yellow solid (27 mg, 51 %). mp 110 – 112 °C. ^{1}H NMR (400 MHz, DMSO-d_6) δ 12.71 (s, 1H), 8.55 (d, J = 1.9 Hz, 1H), 7.99 (d, J = 1.9 Hz, 1H), 7.93 – 7.86 (m, 2H), 7.83 (d, J = 8.3 Hz, 1H), 7.63 (dd, J = 8.3, 1.9 Hz, 1H), 7.44 (d, J = 1.8 Hz, 1H), 7.16 (dd, J = 8.5, 1.6 Hz, 1H), 7.12 (d, J = 8.6 Hz, 1H). ^{13}C NMR (100 MHz, DMSO-d_6) δ 168.8, 144.6, 143.2, 142.4, 138.7, 137.8, 137.4, 136.1, 134.5, 133.6, 133.3, 132.9, 131.8, 130.4, 130.3, 124.6, 123.4, 119.1, 118.1. HRMS (ESI): calcd for $C_{19}H_{10}Cl_3N_2O_6S_2$, $[M-H]^-$ 530.9051, found 530.9033. HPCL purity: 95.31 %.

*2-((4-((3,4-Dichlorophenyl)thio)-3-nitrophenyl)sulfonamido)-4-fluorobenzoic acid (**5e**)*

Yellow solid (34 mg, 66 %). mp 218 – 220 °C. ^{1}H NMR (400 MHz, DMSO-d_6) δ 11.88 (s, 1H), 8.59 (d, J = 2.0 Hz, 1H), 8.00 (d, J = 2.0 Hz, 1H), 7.99 – 7.93 (m, 2H), 7.84 (d, J = 8.3 Hz, 1H), 7.64 (dd, J = 8.3, 2.0 Hz, 1H), 7.23 (dd, J = 10.8, 2.4 Hz, 1H), 7.11 (d, J = 8.7 Hz, 1H), 7.00 (td, J = 8.6, 2.4 Hz, 1H). ^{13}C NMR (100 MHz, DMSO-d_6) δ 169.1, δ 165.3 (d, J = 251.9 Hz), 144.6, 143.8, 142.2, 142.1, 137.4, 136.8, 136.2, 134.9, 134.8, 134.6, 133.3, 133.0, 131.8, 130.33, 130.30, 124.9, 114.9, 111.2 (d, J = 22.3 Hz), 106.16 (d, J = 26.8 Hz). HRMS (ESI): calcd for $C_{19}H_{10}Cl_2FN_2O_6S_2$, $[M-H]^-$ 514.9347, found 514.9360. HPLC purity: 98.91 %.

*2-((4-((3,4-Dichlorophenyl)thio)-3-nitrophenyl)sulfonamido)-5-fluorobenzoic acid (**5f**)*

Yellow solid (32 mg, 62 %). mp 203 – 205 °C. ^{1}H NMR (400 MHz, DMSO-d_6) δ 8.48 (d, J = 1.3 Hz, 1H), 7.98 (d, J = 1.4 Hz, 1H), 7.82 (d, J = 8.2 Hz, 2H), 7.62 (dd, J = 8.3, 1.6 Hz, 1H), 7.56 (dd, J = 9.2, 3.0 Hz, 1H), 7.40 (dd, J = 9.0, 4.8 Hz, 1H), 7.27 (td, J = 8.6, 2.9 Hz, 1H), 7.07 (d, J = 8.6 Hz, 1H). ^{13}C NMR (101 MHz, DMSO-d_6) δ 168.1, 157.5 (d, J = 240.4 Hz), 144.4, 142.3, 139.1, 138.5, 137.4, 136.1, 134.4, 133.3, 132.9, 131.8, 130.6, 130.1, 124.4, 122.9, 121.8 (d, J = 6.4 Hz), 120.5 (d, J = 22.6 Hz), 117.2

(d, J = 23.3 Hz). HRMS (ESI): calcd for $C_{19}H_{10}Cl_2FN_2O_6S_2$, $[M-H]^-$ 514.9347, found 514.9355. HPLC purity: 98.75 %.

*2-((4-((3,4-Dichlorophenyl)thio)-3-nitrophenyl)sulfonamido)-4-(trifluoromethyl)benzoic acid (**5g**)*

Yellow solid (40 mg, 71 %). mp 124 – 126 °C. ^{1}H NMR (400 MHz, DMSO- d_6) δ 14.56 (s, 1H), 8.51 (d, J = 1.4 Hz, 1H), 8.04 (d, J = 8.1 Hz, 1H), 7.98 (d, J = 1.5 Hz, 1H), 7.86 (dd, J = 8.6, 1.4 Hz, 1H), 7.82 (d, J = 8.3 Hz, 1H), 7.69 (s, 1H), 7.62 (dd, J = 8.3, 1.5 Hz, 1H), 7.31 (d, J = 8.0 Hz, 1H), 7.11 (d, J = 8.6 Hz, 1H). ^{13}C NMR (100 MHz, DMSO-d_6) δ 168.1, 144.4, 143.7, 142.3, 139.2, 137.4, 136.1, 134.4, 133.3, 133.2 (q, J = 31.6 Hz), 132.9, 132.8, 131.7, 130.6, 130.3, 124.2, 123.94 (q, J = 271.2 Hz), 123.7, 118.2 (d, J = 3.4 Hz), 115.7 (d, J = 3.9 Hz). HRMS (ESI): calcd for $C_{20}H_{10}Cl_2F_3N_2O_6S_2$, $[M-H]^-$ 564.9315, found 564.9323. HPLC purity: 99.48 %.

*2-((4-((3,4-Dichlorophenyl)thio)-3-nitrophenyl)sulfonamido)-4-methoxybenzoic acid (**5h**)*

Yellow solid (37 mg, 69 %). mp 213 – 215 °C. ^{1}H NMR (400 MHz, DMSO-d_6) δ 11.96 – 11.51 (m, 1H), 8.58 (d, J = 1.9 Hz, 1H), 7.99 (d, J = 1.3 Hz, 1H), 7.94 (dd, J = 8.7, 1.9 Hz, 1H), 7.85 (t, J = 8.5 Hz, 2H), 7.63 (dd, J = 8.3, 1.7 Hz, 1H), 7.12 (d, J = 8.6 Hz, 1H), 6.98 (d, J = 2.2 Hz, 1H), 6.71 (dd, J = 8.9, 2.2 Hz, 1H), 3.79 (s, 3H). ^{13}C NMR (100 MHz, DMSO-d_6) δ 169.9, 164.1, 144.5, 143.9, 141.8, 137.5, 136.7, 136.2, 134.6, 134.1, 133.4, 133.0, 131.9, 130.4, 130.3, 124.9, 110.0, 109.9, 103.8, 56.1. HRMS (ESI): calcd for $C_{20}H_{13}Cl_2N_2O_7S_2$, $[M-H]^-$ 526.9547, found 526.9572. HPLC purity: 95.43 %.

*2-((4-((3,4-Dichlorophenyl)thio)-3-nitrophenyl)sulfonamido)-4,5-dimethoxybenzoic acid (**5i**)*

Yellow solid (34 mg, 61 %). mp 273 – 275 °C. ^{1}H NMR (400 MHz, DMSO-d_6) δ 11.24 (s, 1H), 8.51 (d, *J* = 1.5 Hz, 1H), 7.98 (d, *J* = 1.5 Hz, 1H), 7.82 (dd, *J* = 11.2, 4.8 Hz, 2H), 7.62 (dd, *J* = 8.3, 1.7 Hz, 1H), 7.31 (s, 1H), 7.08 (t, *J* = 4.2 Hz, 2H), 3.82 (s, 3H), 3.72 (s, 3H). ^{13}C NMR (100 MHz, DMSO-d_6) δ 169.5, 153.8, 145.4, 144.5, 143.6, 137.4, 136.6, 136.1, 134.6, 134.3, 133.3, 133.0, 132.0, 130.4, 130.2, 124.8, 113.3, 110.6, 104.0, 56.2, 56.1. HRMS (ESI): calcd for $C_{21}H_{15}Cl_2N_2O_8S_2$, $[M-H]^-$ 556.9652, found 556.9663. HPLC purity: 95.17 %.

*4-Bromo-2-((4-((3,4-dichlorophenyl)thio)-3-nitrophenyl)sulfonamido)benzoic acid (**5j**)*

Yellow solid (43 mg, 75 %). mp 253 – 255 °C.^{1}H NMR (400 MHz, DMSO-d_6) δ 11.49 (s, 1H), 8.56 (d, *J* = 1.9 Hz, 1H), 7.99 (d, *J* = 1.9 Hz, 1H), 7.90 (dd, *J* = 8.7, 2.0 Hz, 1H), 7.82 (dd, *J* = 11.5, 8.4 Hz, 2H), 7.67 – 7.57 (m, 2H), 7.38 (dd, *J* = 8.5, 1.7 Hz, 1H), 7.12 (d, *J* = 8.7 Hz, 1H). ^{13}C NMR (101 MHz, DMSO-d_6) δ 169.1, 144.6, 143.9, 140.5, 137.4, 136.7, 136.1, 134.6, 133.7, 133.4, 133.0, 131.8, 130.4, 130.3, 127.9, 127.5, 124.8, 122.5, 118.3. HRMS (ESI): calcd for $C_{19}H_{10}BrCl_2N_2O_6S_2$, $[M-H]^-$ 574.8546, found 574.8544. HPLC purity: 99.55 %.

*1-((4-((3,4-Dichlorophenyl)thio)-3-nitrophenyl)sulfonamido)cyclopropane-1-carboxylic acid (**5k**)*

Yellow solid (32 mg, 70 %). mp 166 – 168 °C. ^{1}H NMR (400 MHz, DMSO-d_6) δ 8.50 (d, *J* = 1.9 Hz, 1H), 8.02 (d, *J* = 2.0 Hz, 1H), 7.90 – 7.84 (m, 2H), 7.66 (dd, *J* = 8.3, 2.1 Hz, 1H), 7.15 (d, *J* = 8.6 Hz, 1H), 1.29 – 1.21 (m, 2H), 1.13 (dd, *J* = 7.5, 4.4 Hz, 2H).

^{13}C NMR (100 MHz, DMSO-d_6) δ 173.5, 144.4, 141.8, 140.3, 137.3, 136.0, 134.4, 133.3, 132.9, 132.2, 130.8, 129.7, 124.6, 35.6, 16.3. HRMS (ESI): calcd for $C_{16}H_{11}Cl_2N_2O_6S_2$, $[M-H]^-$ 460.9441, found 460.9451. HPLC purity: 93.60 %.

*((4-((3,4-Dichlorophenyl)thio)-3-nitrophenyl)sulfonyl)-L-valine (**5l**)*

Yellow solid (35 mg, 73 %). mp 147 – 149 ℃. ^{1}H NMR (400 MHz, DMSO-d_6) δ 8.55 (d, J = 1.9 Hz, 1H), 8.33 (s, 1H), 8.01 (d, J = 1.9 Hz, 1H), 7.94 – 7.88 (m, 1H), 7.88 – 7.84 (m, 1H), 7.65 (dd, J = 8.3, 2.0 Hz, 1H), 7.15 (d, J = 8.6 Hz, 1H), 3.54 (d, J = 5.6 Hz, 1H), 1.98 (dq, J = 13.2, 6.6 Hz, 1H), 0.84 (d, J = 6.8 Hz, 3H), 0.81 (d, J = 6.8 Hz, 3H). ^{13}C NMR (100 MHz, DMSO-d_6) δ 172.3, 144.4, 141.9, 139.4, 137.2, 136.0, 134.4, 133.3, 132.9, 132.2, 130.8, 129.9, 124.6, 62.0, 30.7, 19.5, 18.2. HRMS (ESI): calcd for $C_{17}H_{15}Cl_2N_2O_6S_2$, $[M-H]^-$ 476.9754, found 476.9759. HPLC purity: 100.00 %.

*((4-((3,4-Dichlorophenyl)thio)-3-nitrophenyl)sulfonyl)-L-phenylalanine (**5m**)*

Yellow solid (41 mg, 77 %). mp 183 – 185 ℃. ^{1}H NMR (400 MHz, DMSO-d_6) δ 8.22 (s, 1H), 8.01 (s, 1H), 7.87 (d, J = 8.3 Hz, 1H), 7.64 (dd, J = 12.0, 9.3 Hz, 2H), 7.07 (s, 5H), 6.93 (d, J = 8.6 Hz, 1H), 3.80 (dd, J = 8.9, 4.0 Hz, 1H), 2.97 (dd, J = 13.6, 4.0 Hz, 1H), 2.71 (dd, J = 13.5, 9.6 Hz, 1H). ^{13}C NMR (100 MHz, DMSO-d_6) δ 172.5, 144.2, 141.7, 139.3, 137.9, 137.4, 136.1, 134.4, 133.3, 132.9, 131.6, 130.7, 129.8, 129.5, 128.2, 126.3, 124.1, 58.6, 38.3. HRMS (ESI): calcd for $C_{21}H_{15}Cl_2N_2O_6S_2$, $[M-H]^-$ 524.9754, found 524.9751. HPLC purity: 99.30 %.

*((4-((3,4-Dichlorophenyl)thio)-3-nitrophenyl)sulfonyl)-L-alanine (**5n**)*

Yellow solid (34 mg, 76 %). mp 133 – 135 ℃. ^{1}H NMR (400 MHz, DMSO-d_6) δ 12.69 (s, 1H), 8.55 (d, J = 1.8 Hz, 2H), 8.02 (d, J = 1.8 Hz, 1H), 7.97 – 7.76 (m, 2H), 7.66 (dd, J = 8.2, 2.0 Hz, 1H), 7.16 (d, J = 8.6 Hz, 1H), 3.83 (d, J = 6.4 Hz, 1H), 1.20 (d, J = 7.1 Hz, 3H). ^{13}C NMR (100 MHz, DMSO-d_6) δ 173.4, 144.5, 142.0, 139.5, 137.3, 136.0, 134.4, 133.3, 132.9, 132.0, 130.8, 130.0, 124.5, 51.8, 18.9. HRMS (ESI): calcd for $C_{15}H_{11}Cl_2N_2O_6S_2$, $[M-H]^-$ 448.9441, found 448.9447. HPLC purity: 97.82 %.

*General procedure for the synthesis of **6a** – **6k***

To a solution of **4c** – **4f** (0.1 mmol) in DMF were added brominated materials (0.15 mmol) and K_2CO_3 (27 mg, 0.2 mmol) at room temperature, the mixture was heated to 80 ℃ overnight. After cooling to ambient temperature, water was added. The mixture was extracted with ethyl acetate. The organic layer was successively washed with water, saturated NaCl aq. Solution, dried over Na_2SO_4 and concentrated. The residue was purified by column chromatography on silica gel to give the titled compounds.

*Methyl 2-((N-(cyclopropylmethyl)-4-((3,4-dichlorophenyl)thio)-3-nitrophenyl)sulfonamido)-5-methylbenzoate (**6a**)*

Yellow solid (50 mg, 86 %); ^{1}H NMR (400 MHz, $CDCl_3$) δ 8.50 (d, J = 1.9 Hz, 1H), 7.70 (d, J = 1.7 Hz, 2H), 7.64 – 7.57 (m, 2H), 7.43 (d, J = 2.0 Hz, 1H), 7.29 (s, 1H), 7.11 (d, J = 8.1 Hz, 1H), 6.90 (d, J = 8.6 Hz, 1H), 3.72 (s, 3H), 3.68 (s, 1H), 3.40 (s, 1H), 2.40 (s, 3H), 1.04 – 0.93 (m, 1H), 0.43 (d, J = 7.8 Hz, 2H), 0.07 (d, J = 24.7 Hz, 2H).

*Methyl 2-((N-benzyl-4-((3,4-dichlorophenyl)thio)-3-nitrophenyl)sulfonamido)-5-methylbenzoate (**6b**)*

Yellow solid (50 mg, 81%); ^{1}H NMR (400 MHz, $CDCl_3$) δ 8.42 (d, *J* = 1.9 Hz, 1H), 7.68 (dd, *J* = 14.0, 1.8 Hz, 2H), 7.61 (d, *J* = 8.3 Hz, 1H), 7.55 (dd, *J* = 8.6, 1.9 Hz, 1H), 7.42 (dd, *J* = 8.3, 2.0 Hz, 1H), 7.21 – 7.28 (m, 5H), 7.16 (dd, *J* = 8.1, 1.6 Hz, 1H), 6.88 (d, *J* = 8.6 Hz, 1H), 6.74 (d, *J* = 8.0 Hz, 1H), 5.06 (s, 1H), 4.63 (s, 1H), 3.70 (s, 3H), 2.34 (s, 3H).

*Methyl 2-((4-((3,4-dichlorophenyl)thio)-N-(4-methoxybenzyl)-3-nitrophenyl)sulfonamido)-5-methylbenzoate (**6c**)*

Yellow solid (55 mg, 85%); ^{1}H NMR (400 MHz, $CDCl_3$) δ 8.41 (d, *J* = 1.7 Hz, 1H), 7.70 (d, *J* = 1.8 Hz, 1H), 7.66 (d, *J* = 1.2 Hz, 1H), 7.60 (d, *J* = 8.3 Hz, 1H), 7.54 (dd, *J* = 8.6, 1.7 Hz, 1H), 7.42 (dd, *J* = 8.3, 1.9 Hz, 1H), 7.15 (dd, *J* = 13.8, 5.0 Hz, 3H), 6.87 (d, *J* = 8.5 Hz, 1H), 6.76 (d, *J* = 8.5 Hz, 2H), 6.70 (d, *J* = 8.0 Hz, 1H), 5.03 (d, *J* = 14.3 Hz, 1H), 4.55 (d, *J* = 14.2 Hz, 1H), 3.77 (s, 3H), 3.71 (s, 3H), 2.34 (s, 3H).

*2-((N-(3-chlorobenzyl)-4-((3,4-dichlorophenyl)thio)-3-nitrophenyl)sulfonamido)-5-methylbenzoic acid (**6d**)*

Yellow solid (50 mg, 74 %); ^{1}H NMR (400 MHz, $CDCl_3$) δ 8.42 (d, *J* = 1.9 Hz, 1H), 7.70 (d, *J* = 2.0 Hz, 1H), 7.67 (d, *J* = 1.6 Hz, 1H), 7.61 (d, *J* = 8.3 Hz, 1H), 7.56 (dd, *J* = 8.5, 2.0 Hz, 1H), 7.43 (dd, *J* = 8.3, 2.0 Hz, 1H), 7.26 – 7.08 (m, 5H), 6.90 (d, *J* = 8.6 Hz, 1H), 6.78 (d, *J* = 8.1 Hz, 1H), 5.02 (s, 1H), 4.62 (s, 1H), 3.70 (s, 3H), 2.36 (s, 3H).

*Methyl 2-((4-((3,4-dichlorophenyl)thio)-3-nitro-N-((5-(p-tolyl)isoxazol-3-yl)methyl)phenyl)sulfonamido)-5-methylbenzoate (**6e**)*

Yellow solid (58 mg, 82%); ^{1}H NMR (400 MHz, $CDCl_3$) δ 8.47 (d, *J* = 1.9 Hz, 1H), 7.69 (s, 2H), 7.65 (d, *J* = 8.1 Hz, 2H), 7.63 – 7.60 (m, 1H), 7.60 – 7.58 (m, 1H), 7.41 (dd, *J* = 8.3, 2.0 Hz, 1H), 7.29 (s, 1H), 7.23 (dd, *J* = 8.1, 1.6 Hz, 1H), 6.98 (d, *J* = 8.1 Hz, 1H), 6.91 (d, *J* = 8.6 Hz, 1H), 6.70 (s, 1H), 5.18 (d, *J* = 15.8 Hz, 1H), 4.75 (d, *J* = 15.3 Hz, 1H), 3.71 (s, 3H), 2.41 (s, 3H), 2.36 (s, 3H).

*Methyl 2-((N-(cyclopropylmethyl)-4-((3,4-dichlorophenyl)thio)-3-nitrophenyl)sulfonamido)-4-fluorobenzoate (**6f**)*

Yellow solid (40 mg, 68 %); ^{1}H NMR (400 MHz, $CDCl_3$) δ 8.53 (d, *J* = 1.9 Hz, 1H), 7.95 (dd, *J* = 8.8, 6.4 Hz, 1H), 7.70 (d, *J* = 1.9 Hz, 1H), 7.63 – 7.57 (m, 2H), 7.43 (dd, *J* = 8.3, 2.0 Hz, 1H), 7.19 – 7.13 (m, 1H), 7.01 (dd, *J* = 9.0, 2.5 Hz, 1H), 6.93 (d, *J* = 8.6 Hz, 1H), 3.72 (s, 4H), 3.39 (s, 1H), 1.04 – 0.94 (m, 1H), 0.46 (d, *J* = 7.9 Hz, 2H), 0.08 (d, *J* = 27.8 Hz, 2H).

*Methyl 2-((4-((3,4-dichlorophenyl)thio)-3-nitro-N-((5-(p-tolyl)isoxazol-3-yl)methyl)phenyl)sulfonamido)-4-fluorobenzoate (**6g**)*

Yellow solid (50 mg, 71 %); ^{1}H NMR (400 MHz, $CDCl_3$) δ 8.50 (d, *J* = 1.9 Hz, 1H), 7.95 (dd, *J* = 8.8, 6.3 Hz, 1H), 7.70 (d, *J* = 2.0 Hz, 1H), 7.66 (d, *J* = 8.1 Hz, 2H), 7.60 (dd, *J* = 8.5, 2.2 Hz, 2H), 7.41 (dd, *J* = 8.3, 2.0 Hz, 1H), 7.28 (d, *J* = 8.5 Hz, 2H), 7.14 (ddd, *J* = 8.9, 7.5, 2.6 Hz, 1H), 6.93 (dd, *J* = 8.7, 1.4 Hz, 2H), 6.68 (s, 1H), 5.17 (s, 1H), 4.78 (s, 1H), 3.72 (s, 3H), 2.42 (s, 3H).

*Methyl 4-chloro-2-((4-((3,4-dichlorophenyl)thio)-3-nitro-N-((5-(p-tolyl)isoxazol-3-yl)methyl)phenyl)sulfonamido)benzoate (**6h**)*

Yellow solid (55 mg, 76 %); ^{1}H NMR (400 MHz, $CDCl_3$) δ 8.49 (d, *J* = 2.0 Hz, 1H), 7.86 (d, *J* = 8.4 Hz, 1H), 7.70 (d, *J* = 1.9 Hz, 1H), 7.66 (d, *J* = 8.1 Hz, 2H), 7.62 – 7.56 (m, 2H), 7.42 (dd, *J* = 8.3, 2.0 Hz, 2H), 7.29 (d, *J* = 8.1 Hz, 2H), 7.16 (d, *J* = 2.0 Hz, 1H), 6.93 (d, *J* = 8.6 Hz, 1H), 6.68 (s, 1H), 5.13 (s, 1H), 4.76 (s, 1H), 3.74 (s, 3H), 2.42 (s, 3H).

*Methyl 4-chloro-2-((N-(cyclopropylmethyl)-4-((3,4-dichlorophenyl)thio)-3-nitrophenyl)sulfonamido)benzoate (**6i**)*

Yellow solid (42 mg, 70 %); ^{1}H NMR (400 MHz, $CDCl_3$) δ 8.53 (d, *J* = 1.9 Hz, 1H), 7.86 (d, *J* = 8.5 Hz, 1H), 7.70 (d, *J* = 2.0 Hz, 1H), 7.64 – 7.56 (m, 2H), 7.46 – 7.40 (m, 2H), 7.23 (d, *J* = 2.0 Hz, 1H), 6.93 (d, *J* = 8.6 Hz, 1H), 3.74 (s, 3H), 3.67 (s, 1H), 3.41 (s, 1H), 1.05 – 0.93 (m, 1H), 0.47 (d, *J* = 7.8 Hz, 2H), 0.08 (d, *J* = 27.4 Hz, 2H).

*Methyl 2-((N-(cyclopropylmethyl)-4-((3,4-dichlorophenyl)thio)-3-nitrophenyl)sulfonamido)-5-fluorobenzoate (**6j**)*

Yellow solid (42 mg, 70 %); ^{1}H NMR (400 MHz, $CDCl_3$) δ 8.52 (d, *J* = 1.9 Hz, 1H), 7.70 (d, *J* = 2.0 Hz, 1H), 7.66 – 7.53 (m, 3H), 7.42 (dd, *J* = 8.3, 2.0 Hz, 1H), 7.26 – 7.13 (m, 2H), 6.92 (d, *J* = 8.6 Hz, 1H), 3.77 – 3.68 (m, 4H), 3.38 (dd, *J* = 14.0, 7.3 Hz, 1H), 0.97 (qd, *J* = 7.5, 3.7 Hz, 1H), 0.43 (t, *J* = 9.6 Hz, 2H), 0.07 (d, *J* = 35.8 Hz, 2H).

*Methyl 2-((4-((3,4-dichlorophenyl)thio)-3-nitro-N-((5-(p-tolyl)isoxazol-3-yl)methyl)phenyl)sulfonamido)-5-fluorobenzoate (**6k**)*

Yellow solid (65mg, 93 %); ^{1}H NMR (400 MHz, $CDCl_3$) δ 8.49 (d, *J* = 2.0 Hz, 1H), 7.69 (d, *J* = 2.0 Hz, 1H), 7.65 (d, *J* = 8.1 Hz, 2H), 7.63 – 7.55 (m, 3H), 7.41 (dd, *J* = 8.3, 2.0 Hz, 1H), 7.28 (d, *J* = 8.0 Hz, 2H), 7.13 (dd, *J* = 6.0, 1.5 Hz, 2H), 6.92 (d, *J* = 8.7 Hz, 1H), 6.67 (s, 1H), 5.21 (d, *J* = 16.1 Hz, 1H), 4.73 (d, *J* = 16.3 Hz, 1H), 3.74 (s, 3H), 2.42 (s, 3H).

*General procedure for the synthesis of **7a** – **7k***

The methyl esters of the title compounds (**6a** – **6k**) (0.1 mmol) were hydrolyzed with 1 M NaOH in dioxane (1:1) at 50 ℃ overnight. The mixture was then diluted with a small amount of water and washed twice with DCM. The aqueous solution was acidified by the addition of 2 M HCl. The precipitate was collected by filtration and washed with water to provide the title compounds (**7a** – **7k**).

*2-((N-(cyclopropylmethyl)-4-((3,4-dichlorophenyl)thio)-3-nitrophenyl)sulfonamido)-5-methylbenzoic acid (**7a**)*

Yellow solid (35 mg, 62 %). mp 207 – 209 ℃. ^{1}H NMR (400 MHz, $CDCl_3$) δ 8.55 (d, *J* = 1.8 Hz, 1H), 7.84 (d, *J* = 1.3 Hz, 1H), 7.66 (d, *J* = 1.9 Hz, 1H), 7.61 – 7.50 (m, 2H), 7.42 – 7.32 (m, 2H), 7.14 (d, *J* = 8.1 Hz, 1H), 6.91 (d, *J* = 8.6 Hz, 1H), 3.70 (dd, *J* = 14.1, 6.7 Hz, 1H), 3.41 (dd, *J* = 14.1, 7.4 Hz, 1H), 2.44 (s, 3H), 1.04 – 0.93 (m, 1H), 0.51 – 0.40 (m, 2H), 0.10 (d, *J* = 30.6 Hz, 2H). ^{13}C NMR (100 MHz, $CDCl_3$) δ 169.5, 144.3, 143.4, 139.7, 137.6, 137.1, 135.7, 135.4, 134.8, 134.5, 134.2, 133.2, 132.3, 131.6, 129.7, 129.6, 128.4, 125.2, 57.5, 21.1, 10.4, 4.4, 3.8. HRMS (ESI): calcd for $C_{24}H_{19}Cl_2N_2O_6S_2$, $[M-H]^-$ 565.0067, found 565.0053. HPLC purity: 98.98 %.

*2-((N-benzyl-4-((3,4-dichlorophenyl)thio)-3-nitrophenyl)sulfonamido)-5-methylbenzoic acid (**7b**)*

Yellow solid (32 mg, 53 %). mp 145 – 147 °C. ^{1}H NMR (400 MHz, $CDCl_3$) δ 8.52 (d, *J* = 1.6 Hz, 1H), 7.81 (s, 1H), 7.65 (d, *J* = 1.9 Hz, 1H), 7.55 (d, *J* = 8.2 Hz, 1H), 7.51 (dd, *J* = 8.6, 1.7 Hz, 1H), 7.37 (dd, *J* = 8.2, 2.0 Hz, 1H), 7.28 – 7.20 (m, 6H), 6.88 (d, *J* = 8.6 Hz, 1H), 6.78 (d, *J* = 8.0 Hz, 1H), 5.13 (d, *J* = 14.5 Hz, 1H), 4.62 (d, *J* = 14.5 Hz, 1H), 2.39 (s, 3H). ^{13}C NMR (100 MHz, $CDCl_3$) δ 169.7, 144.4, 143.3, 139.6, 137.9, 137.1, 135.7, 135.5, 135.0, 134.8, 134.5, 134.3, 133.3, 133.0, 132.3, 131.6, 129.8, 129.5, 128.6, 128.4, 128.2, 125.3, 56.4, 21.0. HRMS (ESI): calcd for $C_{27}H_{19}Cl_2N_2O_6S_2$, $[M-H]^-$ 601.0067, found 601.0046. HPLC purity: 98.42 %

*2-((4-((3,4-Dichlorophenyl)thio)-N-(4-methoxybenzyl)-3-nitrophenyl)sulfonamido)-5-methylbenzoic acid (**7c**)*

Yellow solid (42 mg, 66 %). mp 143 – 145 °C. ^{1}H NMR (400 MHz, $CDCl_3$) δ 8.51 (d, *J* = 1.7 Hz, 1H), 7.82 (s, 1H), 7.64 (d, *J* = 1.9 Hz, 1H), 7.54 (d, *J* = 8.3 Hz, 1H), 7.50 (dd, *J* = 8.5, 1.7 Hz, 1H), 7.36 (dd, *J* = 8.3, 1.9 Hz, 1H), 7.23 (d, *J* = 8.0 Hz, 1H), 7.16 (d, *J* = 8.4 Hz, 2H), 6.87 (d, *J* = 8.6 Hz, 1H), 6.76 (t, *J* = 8.8 Hz, 3H), 5.08 (d, *J* = 14.6 Hz, 1H), 4.55 (d, *J* = 14.6 Hz, 1H), 3.77 (s, 3H), 2.40 (s, 3H). ^{13}C NMR (100 MHz, $CDCl_3$) δ 170.2, 159.4, 144.3, 143.2, 139.6, 138.1, 137.1, 135.6, 135.0, 134.8, 134.5, 134.3, 133.3, 133.1, 132.3, 131.6, 130.9, 129.8, 129.1, 128.4, 127.5, 125.2, 113.8, 55.9, 55.2, 21.1. HRMS (ESI): calcd for $C_{28}H_{21}Cl_2N_2O_7S_2$, $[M-H]^-$ 631.0173, found 631.0180. HPLC purity: 99.12 %.

*2-((N-(3-chlorobenzyl)-4-((3,4-dichlorophenyl)thio)-3-nitrophenyl)sulfonamido)-5-methylbenzoic acid (**7d**)*

Yellow solid (42 mg, 66 %). mp 129 – 131 °C. ^{1}H NMR (400 MHz, $CDCl_3$) δ 8.52 (d, *J* = 1.9 Hz, 1H), 7.83 (d, *J* = 1.4 Hz, 1H), 7.66 (d, *J* = 1.9 Hz, 1H), 7.56 (d, *J* = 8.3 Hz, 1H), 7.51 (dd, *J* = 8.6, 1.9 Hz, 1H), 7.38 (dd, *J* = 8.3, 2.0 Hz, 1H), 7.29 (d, *J* = 1.3 Hz, 1H), 7.26 – 7.15 (m, 4H), 6.90 (d, *J* = 8.6 Hz, 1H), 6.83 (d, *J* = 8.1 Hz, 1H), 5.10 (d, *J* = 15.0 Hz, 1H), 4.58 (d, *J* = 15.0 Hz, 1H), 2.41 (s, 3H). ^{13}C NMR (100 MHz, $CDCl_3$) δ 169.6, 144.3, 143.6, 139.9, 137.73, 137.71, 137.1, 135.7, 134.9, 134.8, 134.5, 134.4, 133.5, 133.0, 132.3, 131.6, 129.9, 129.7, 129.4, 128.7, 128.4, 128.3, 127.6, 125.3, 55.8, 21.1. HRMS (ESI): calcd for $C_{27}H_{18}Cl_3N_2O_6S_2$, $[M-H]^-$ 634.9677, found 634.9681. HPLC purity: 96.91 %.

*2-((4-((3,4-Dichlorophenyl)thio)-3-nitro-N-((5-(p-tolyl)isoxazol-3-yl)methyl)phenyl)sulfonamido)-5-methylbenzoic acid (**7e**)*

Yellow solid (40 mg, 58%); mp 191 – 193 °C. ^{1}H NMR (400 MHz, $CDCl_3$) δ 8.54 (d, *J* = 1.8 Hz, 1H), 7.79 (d, *J* = 1.1 Hz, 1H), 7.65 (dd, *J* = 11.2, 5.0 Hz, 3H), 7.57 (td, *J* = 8.1, 3.9 Hz, 2H), 7.38 (dd, *J* = 8.3, 1.9 Hz, 1H), 7.30 – 7.26 (m, 3H), 6.99 (d, *J* = 8.1 Hz, 1H), 6.93 (d, *J* = 8.6 Hz, 1H), 6.64 (s, 1H), 5.08 (d, *J* = 16.2 Hz, 1H), 4.85 (d, *J* = 16.0 Hz, 1H), 2.40 (s, 6H). ^{13}C NMR (100 MHz, DMSO-d_6) δ 169.9, 167.1, 161.2, 144.6, 143.1, 140.9, 139.6, 137.2, 135.9, 134.8, 134.4, 133.6, 133.3, 132.9, 132.4, 132.3, 132.0, 130.7, 130.3, 130.0, 126.0, 125.1, 124.4, 100.1, 47.7, 21.5, 20.9. HRMS (ESI): calcd for $C_{31}H_{22}Cl_2N_3O_7S_2$, $[M-H]^-$ 682.0282, found 682.0290. HPLC purity: 97.92 %.

*2-((N-(cyclopropylmethyl)-4-((3,4-dichlorophenyl)thio)-3-nitrophenyl)sulfonamido)-4-fluorobenzoic acid (**7f**)*

Yellow solid (31 mg, 53 %). mp 136 – 138 °C. ^{1}H NMR (400 MHz, $CDCl_3$) δ 8.59 (d, *J* = 1.4 Hz, 1H), 8.13 – 8.02 (m, 1H), 7.66 (d, *J* = 1.8 Hz, 1H), 7.57 (t, *J* = 9.1 Hz, 2H),

7.39 (dd, *J* = 8.3, 1.8 Hz, 1H), 7.26 – 7.18 (m, 1H), 7.05 (d, *J* = 8.4 Hz, 1H), 6.92 (d, *J* = 8.6 Hz, 1H), 3.72 (s, 1H), 3.42 (s, 1H), 0.99 (s, 1H), 0.48 (d, *J* = 7.9 Hz, 2H), 0.10 (d, *J* = 39.8 Hz, 2H). ^{13}C NMR (100 MHz, $CDCl_3$) δ 168.3, 164.9 (d, *J* = 257.3 Hz), 144.3, 143.8, 140.7 (d, *J* = 10.9 Hz), 137.4, 137.2, 135.8, 134.85, 134.80, 134.76, 134.6, 132.4, 131.5, 129.6, 128.5, 125.2, 120.4 (d, *J* = 22.1 Hz), 116.5 (d, *J* = 20.9 Hz), 57.4, 10.3, 4.5, 3.7. HRMS (ESI): calcd for $C_{23}H_{16}Cl_2FN_2O_6S_2$, $[M-H]^-$ 568.9816, found 568.9799. HPLC purity: 97.97 %.

*2-((4-((3,4-Dichlorophenyl)thio)-3-nitro-N-((5-(p-tolyl)isoxazol-3-yl)methyl)phenyl)sulfonamido)-4-fluorobenzoic acid (7**g**)*

Yellow solid (41 mg, 60 %). mp 153 – 155 °C. ^{1}H NMR (400 MHz, DMSO-d_6) δ 13.15 (s, 1H), 8.35 (d, *J* = 1.9 Hz, 1H), 8.00 – 7.89 (m, 2H), 7.84 (d, *J* = 8.3 Hz, 1H), 7.69 (d, *J* = 8.1 Hz, 2H), 7.64 (ddd, *J* = 16.7, 8.6, 2.0 Hz, 2H), 7.40 (dd, *J* = 8.3, 2.3 Hz, 1H), 7.36 (d, *J* = 8.0 Hz, 2H), 7.24 (dd, *J* = 9.5, 2.3 Hz, 1H), 7.10 (d, *J* = 8.6 Hz, 1H), 6.93 (s, 1H), 5.11 (d, *J* = 14.5 Hz, 1H), 4.83 (d, *J* = 14.6 Hz, 1H), 2.38 (s, 3H). ^{13}C NMR (100 MHz, DMSO-d_6) δ 169.9, 166.1, 163.8 (d, *J* = 250 Hz), 161.0, 144.7, 143.3, 140.9, 137.2, 136.6, 135.9, 134.5, 134.3, 134.2 (*d*, = 10 Hz), 133.4, 132.9, 132.4, 130.7, 130.3, 130.0, 129.1, 126.0, 125.3, 124.4, 119.4 (d, J = 23 Hz), 116.9 (d, *J* = 21 Hz), 100.1, 47.6, 21.5. HRMS (ESI): calcd for $C_{30}H_{19}Cl_2FN_3O_7S_2$, $[M-H]^-$ 686.0031, found 686.0015. HPLC purity: 92.97 %.

*4-Chloro-2-((4-((3,4-dichlorophenyl)thio)-3-nitro-N-((5-(p-tolyl)isoxazol-3-yl)methyl)phenyl)sulfonamido)benzoic acid (7**h**)*

Yellow solid (47 mg, 66 %). mp 241 – 243 °C. ^{1}H NMR (400 MHz, DMSO-d_6) δ 8.38 (s, 1H), 7.99 (s, 1H), 7.81 (t, *J* = 7.5 Hz, 2H), 7.72 (d, *J* = 7.8 Hz, 2H), 7.69 – 7.56 (m,

2H), 7.35 (d, *J* = 7.4 Hz, 3H), 7.18 (s, 1H), 7.07 (d, *J* = 8.6 Hz, 1H), 6.98 (s, 1H), 5.07 (s, 2H), 2.38 (s, 3H). ^{13}C NMR (100 MHz, DMSO-d_6) δ 169.8, 167.6, 161.9, 144.6, 142.4, 140.8, 137.5, 137.0, 136.7, 135.8, 134.2, 133.3, 133.0, 132.8, 132.7, 131.9, 131.1, 130.2, 129.6, 128.9, 126.0, 125.8, 124.5, 100.0, 47.6, 21.5. HRMS (ESI): calcd for $C_{30}H_{19}Cl_3N_3O_7S_2$, $[M-H]^-$ 701.9735, found 701.9742. HPLC purity: 99.04 %.

*4-Chloro-2-((N-(cyclopropylmethyl)-4-((3,4-dichlorophenyl)thio)-3-nitrophenyl)sulfonamido)benzoic acid (**7i**)*

Yellow solid (36 mg, 61 %). mp 115 – 117 °C. ^{1}H NMR (400 MHz, $CDCl_3$) δ 8.58 (d, *J* = 1.6 Hz, 1H), 7.99 (d, *J* = 8.5 Hz, 1H), 7.67 (d, *J* = 1.8 Hz, 1H), 7.59 (d, *J* = 8.3 Hz, 1H), 7.54 (dd, *J* = 8.6, 1.3 Hz, 1H), 7.49 (d, *J* = 8.3 Hz, 1H), 7.40 (dd, *J* = 8.2, 1.8 Hz, 1H), 7.23 (s, 1H), 6.93 (d, *J* = 8.6 Hz, 1H), 3.68 (dd, *J* = 13.8, 6.9 Hz, 1H), 3.41 (dd, *J* = 13.9, 6.9 Hz, 1H), 1.06 – 0.89 (m, 1H), 0.48 (d, *J* = 7.8 Hz, 2H), 0.21 – 0.01 (m, 2H). ^{13}C NMR (100 MHz, $CDCl_3$) δ 168.1, 150.7, 144.4, 143.9, 139.4, 139.3, 137.1, 135.8, 134.8, 134.6, 133.6, 132.7, 132.4, 131.6, 129.6, 129.5, 128.5, 125.2, 57.4, 10.3, 4.4, 3.9. HRMS (ESI): calcd for $C_{23}H_{16}Cl_3N_2O_6S_2$, $[M-H]^-$ 584.9521, found 584.9504. HPLC purity: 96.65 %.

*2-((N-(cyclopropylmethyl)-4-((3,4-dichlorophenyl)thio)-3-nitrophenyl)sulfonamido)-5-fluorobenzoic acid (**7j**)*

Yellow solid (27 mg, 52 %). mp 69 – 71 °C. ^{1}H NMR (400 MHz, $CDCl_3$) δ 8.56 (d, *J* = 1.8 Hz, 1H), 7.72 (d, *J* = 8.5 Hz, 1H), 7.67 (d, *J* = 1.9 Hz, 1H), 7.59 (d, *J* = 8.3 Hz, 1H), 7.56 (dd, *J* = 8.7, 1.9 Hz, 1H), 7.40 (dd, *J* = 8.3, 1.9 Hz, 1H), 7.28 (dd, *J* = 6.1, 1.4 Hz, 2H), 6.92 (d, *J* = 8.6 Hz, 1H), 3.73 (dd, *J* = 14.2, 6.9 Hz, 1H), 3.40 (dd, *J* = 14.2, 7.5 Hz, 1H), 0.98 (dt, *J* = 7.5, 4.9 Hz, 1H), 0.46 (t, *J* = 9.5 Hz, 2H), 0.19 – 0.01 (m, 2H).

^{13}C NMR (100 MHz, $CDCl_3$) δ 168.0, 161.9 (d, *J* = 250.6 Hz), 144.4, 143.7, 137.5, 137.2, 135.8, 134.8, 134.6, 134.5, 134.1 (d, *J* = 4.0 Hz), 132.4, 132.0 (d, *J* = 8.0 Hz), 131.5, 129.6, 128.5, 125.2, 120.5 (d , *J* = 23.0 Hz), 119.5 (d, *J* = 25.0 Hz), 57.5, 10.3, 4.4, 3.8. HRMS (ESI): calcd for $C_{23}H_{16}Cl_2FN_2O_6S_2$, $[M-H]^-$ 568.9816, found 568.9819. HPLC purity: 100.00 %.

*2-((4-((3,4-Dichlorophenyl)thio)-3-nitro-N-((5-(p-tolyl)isoxazol-3-yl)methyl)phenyl)sulfonamido)-5-fluorobenzoic acid (**7k**)*

Yellow solid (36 mg, 53 %). mp 285 – 287. ^{1}H NMR (400 MHz, DMSO-d_6) δ 8.37 (d, *J* = 1.9 Hz, 1H), 8.01 (d, *J* = 1.8 Hz, 1H), 7.86 – 7.76 (m, 2H), 7.72 (d, *J* = 8.1 Hz, 2H), 7.66 (dd, *J* = 8.3, 1.8 Hz, 1H), 7.35 (d, *J* = 8.0 Hz, 2H), 7.27 (d, *J* = 7.7 Hz, 1H), 7.15 – 7.00 (m, 3H), 6.92 (s, 1H), 5.07 (s, 2H), 2.38 (s, 3H). ^{13}C NMR (100 MHz, DMSO-d_6) δ 169.7, 167.1, 161.8 (d, *J* = 245.0 Hz), 161.9, 144.6, 142.3, 140.8, 137.8, 137.0, 135.8, 134.84, 134.76, 134.2, 133.2, 132.9, 132.8, 131.5, 131.2, 130.2, 129.7, 126.0, 125.7, 124.5, 117.1 (d, *J* = 22.9 Hz), 115.4 (d, *J* = 23.0 Hz), 100.0, 47.6, 21.5. HRMS (ESI): calcd for $C_{30}H_{19}Cl_2FN_3O_7S_2$, $[M-H]^-$ 686.0031, found 686.0036. HPLC purity: 99.48 %.

*Synthesis of methyl 2-((N-(3-bromopropyl)-4-((3,4-dichlorophenyl)thio)-3-nitrophenyl)sulfonamido)-5-methylbenzoate (**8**)*

To a solution of **4c** (2.64 g, 5 mmol) in DMF in acetone were added 1,4-dibromobutane (7.5 mmol) and K_2CO_3 (1.38g, 10 mmol) at room temperature, the mixture was heated to 60 ℃ overnight. After cooling to ambient temperature, water was added. The mixture was extracted with ethyl acetate. The organic layer was successively washed with water, saturated NaCl aq. Solution, dried over Na_2SO_4 and concentrated. The residue was

purified by column chromatography on silica gel to give the titled compound, yellow jelly (2.33 g, 72 %); ^{1}H NMR (400 MHz, $CDCl_3$) δ 8.43 (d, *J* = 1.8 Hz, 1H), 7.70 (d, *J* = 1.9 Hz, 2H), 7.61 (d, *J* = 8.3 Hz, 1H), 7.55 (dd, *J* = 8.6, 1.9 Hz, 1H), 7.42 (dd, *J* = 8.3, 1.9 Hz, 1H), 7.30 (dd, *J* = 8.0, 1.5 Hz, 1H), 6.98 (d, *J* = 8.1 Hz, 1H), 6.91 (d, *J* = 8.6 Hz, 1H), 3.74 (s, 3H), 3.65 (dd, *J* = 16.0, 6.9 Hz, 2H), 3.38 (d, *J* = 3.8 Hz, 2H), 2.40 (s, 3H), 1.99 – 1.86 (m, 2H), 1.71 (dt, *J* = 14.7, 7.3 Hz, 2H).

*General procedure for the synthesis of compound **9a** – **9d***

To a solution of **8** (133 mg, 0.2 mmol) in DMF in acetone were added amine (0.3 mmol) and K_2CO_3 (55 mg, 0.4mmol) at room temperature, the mixture was heated to 40 ℃ overnight. After cooling to ambient temperature, water was added. The mixture was extracted with ethyl acetate. The organic layer was successively washed with water, saturated NaCl aqueous solution, dried over Na_2SO_4 and concentrated. The residue was purified by column chromatography on silica gel to give compound ***9a*** – ***9d***.

*Methyl 2-((4-((3,4-dichlorophenyl)thio)-N-(4-(diethylamino)butyl)-3-nitrophenyl)sulfonamido)-5-methylbenzoate (**9a**)*

Yellow solid (120 mg, 92 %). ^{1}H NMR (400 MHz, $CDCl_3$) δ 8.39 (d, *J* = 1.8 Hz, 1H), 7.71 (d, *J* = 1.9 Hz, 1H), 7.68 (s, 1H), 7.62 (d, *J* = 8.3 Hz, 1H), 7.52 (dd, *J* = 8.6, 1.9 Hz, 1H), 7.44 (dd, *J* = 8.3, 2.0 Hz, 1H), 7.30 (d, *J* = 1.7 Hz, 1H), 6.91 (dd, *J* = 10.6, 8.5 Hz, 2H), 3.77 (s, 3H), 3.71 – 3.55 (m, 2H), 2.97 (d, *J* = 5.9 Hz, 4H), 2.84 (s, 2H), 2.40 (s, 3H), 1.71 – 1.56 (m, 4H), 1.33 – 1.28 (m, 6H).

*Methyl 2-((4-((3,4-dichlorophenyl)thio)-3-nitro-N-(4-(pyrrolidin-1-yl)butyl)phenyl)sulfonamido)-5-methylbenzoate (**9b**)*

Yellow solid (70 mg, 54 %). ^{1}H NMR (400 MHz, $CDCl_3$) δ 8.42 (d, *J* = 1.8 Hz, 1H), 7.70 (dd, *J* = 5.6, 1.7 Hz, 2H), 7.61 (d, *J* = 8.3 Hz, 1H), 7.55 (dd, *J* = 8.6, 1.9 Hz, 1H), 7.43 (dd, *J* = 8.3, 2.0 Hz, 1H), 7.29 (dd, *J* = 8.2, 1.6 Hz, 1H), 6.93 (dd, *J* = 12.1, 8.4 Hz, 2H), 3.75 (s, 3H), 3.63 (t, *J* = 7.1 Hz, 2H), 2.71 (d, *J* = 48.5 Hz, 6H), 2.40 (s, 3H), 1.90 (s, 4H), 1.71 (s, 2H), 1.66 – 1.59 (m, 2H).

*Methyl 2-((4-((3,4-dichlorophenyl)thio)-N-(4-(3,3-difluoropyrrolidin-1-yl)butyl)-3-nitrophenyl)sulfonamido)-5-methylbenzoate (**9c**)*

Yellow solid (90 mg, 65 %). ^{1}H NMR (400 MHz, $CDCl_3$) δ 8.43 (d, *J* = 1.6 Hz, 1H), 7.70 (d, *J* = 1.8 Hz, 2H), 7.61 (d, *J* = 8.3 Hz, 1H), 7.55 (d, *J* = 8.4 Hz, 1H), 7.42 (dd, *J* = 8.3, 2.0 Hz, 1H), 7.30 (dd, *J* = 8.1, 1.5 Hz, 1H), 6.98 (d, *J* = 8.1 Hz, 1H), 6.91 (d, *J* = 8.6 Hz, 1H), 4.05 (d, *J* = 5.6 Hz, 2H), 3.73 (s, 3H), 3.69 – 3.47 (m, 6H), 2.40 (s, 3H), 2.33 (td, *J* = 13.3, 6.8 Hz, 2H), 1.66 (s, 4H).

*Methyl 2-((4-((3,4-dichlorophenyl)thio)-N-(4-morpholinobutyl)-3-nitrophenyl)sulfonamido)-5-methylbenzoate (**9d**)*

Yellow solid (104 mg, 78 %). ^{1}H NMR (400 MHz, $CDCl_3$) δ 8.45 (d, *J* = 1.6 Hz, 1H), 7.70 (d, *J* = 1.5 Hz, 2H), 7.61 (d, *J* = 8.2 Hz, 1H), 7.55 (dd, *J* = 8.7, 1.8 Hz, 1H), 7.42 (dd, *J* = 8.3, 1.9 Hz, 1H), 7.30 (d, *J* = 8.0 Hz, 1H), 6.99 (d, *J* = 8.1 Hz, 1H), 6.90 (d, *J* = 8.6 Hz, 1H), 3.74 (s, 3H), 3.69 – 3.58 (m, 6H), 2.40 (s, 3H), 2.37 (s, 4H), 2.31 – 2.25 (m, 2H), 1.58 – 1.63 (m, 2H), 1.47 (dt, *J* = 14.0, 7.1 Hz, 2H).

*General procedure for the synthesis of **10a** – **10d***

The methyl esters of the title compounds (**9a** – **9d**) (0.1 mmol) were hydrolyzed with 1 M NaOH in dioxane (1 : 1) at 50 °C overnight. The mixture was then diluted with a small amount of water and washed twice with DCM. The aqueous solution was acidified by the addition of 2 M HCl. The precipitate was collected by filtration and washed with water to provide the title compounds **10a** – **10d**.

*2-((4-((3,4-dichlorophenyl)thio)-N-(4-(diethylamino)butyl)-3-nitrophenyl)sulfonamido)-5-methylbenzoic acid (**10a**)*

Yellow solid (15 mg, 23 %). mp 196 – 198 °C. ^{1}H NMR (400 MHz, DMSO-d_6) δ 8.32 (d, J = 1.6 Hz, 1H), 8.01 (d, J = 1.9 Hz, 1H), 7.87 (d, J = 8.3 Hz, 1H), 7.67 (td, J = 8.4, 1.6 Hz, 2H), 7.50 (s, 1H), 7.25 (d, J = 7.9 Hz, 1H), 7.10 (d, J = 8.6 Hz, 1H), 6.98 (d, J = 8.1 Hz, 1H), 3.60 – 3.50 (m, 2H), 2.82 (q, J = 6.3 Hz, 4H), 2.71 (s, 2H), 2.32 (s, 3H), 1.55 – 1.40 (m, 4H), 1.07 (t, J = 7.1 Hz, 6H). ^{13}C NMR (100 MHz, DMSO-*d*6) δ 168.0, 144.1, 141.9, 138.0, 136.6, 135.4, 133.9, 133.2, 132.8, 132.4, 132.0, 131.1, 130.8, 130.2, 130.1, 129.24, 129.19, 124.7, 50.7, 50.6, 46.0, 45.9, 25.4, 21.3, 20.4, 9.2, 9.1. HRMS (ESI): calcd for $C_{28}H_{30}Cl_2N_3O_6S_2$, $[M-H]^-$ 638.0959, found 638.0968. HPLC purity: 93.37 %.

*2-((4-((3,4-Dichlorophenyl)thio)-3-nitro-N-(4-(pyrrolidin-1-yl)butyl)phenyl)sulfonamido)-5-methylbenzoic acid (**10b**)*

Yellow solid (52 mg, 41 %). mp 221 – 223 °C. ^{1}H NMR (400 MHz, $CDCl_3$) δ 8.54 (d, J = 1.8 Hz, 1H), 7.70 (d, J = 1.9 Hz, 1H), 7.64 – 7.56 (m, 3H), 7.44 (dd, J = 8.2, 2.0 Hz, 1H), 7.11 (d, J = 8.1 Hz, 1H), 6.93 (d, J = 8.6 Hz, 1H), 6.80 (d, J = 8.0 Hz, 1H), 3.64 (s, 2H), 3.23 (s, 6H), 3.00 – 2.94 (m, 2H), 2.34 (s, 3H), 2.04 (s, 4H), 1.66 – 1.52 (m,

2H). ^{13}C NMR (100 MHz, $CDCl_3$) δ 170.9, 144.3, 143.0, 138.9, 137.5, 137.3, 137.1, 135.6, 134.9, 134.4, 133.2, 132.3, 132.1, 131.7, 130.9, 129.8, 129.0, 128.4, 125.5, 55.0, 53.5, 51.3, 25.7, 23.3, 23.0, 21.0. HRMS (ESI): calcd for $C_{28}H_{28}Cl_2N_3O_6S_2$, $[M-H]^-$ 636.0802, found 636.0811. HPCL purity: 97.78 %.

*2-((4-((3,4-Dichlorophenyl)thio)-N-(4-(3,3-difluoropyrrolidin-1-yl)butyl)-3-nitrophenyl)sulfonamido)-5-methylbenzoic acid (**10c**)*

Yellow solid (54 mg, 40 %). mp 98 – 100 °C. 1H NMR (400 MHz, $CDCl_3$) δ 8.50 (s, 1H), 7.83 (s, 1H), 7.66 (d, *J* = 1.5 Hz, 1H), 7.56 (d, *J* = 8.3 Hz, 1H), 7.51 (d, *J* = 8.4 Hz, 1H), 7.44 – 7.32 (m, 2H), 7.04 (d, *J* = 7.9 Hz, 1H), 6.91 (d, *J* = 8.6 Hz, 1H), 4.06 (s, 2H), 3.75 – 3.49 (m, 6H), 2.43 (s, 3H), 2.32 (dd, *J* = 12.6, 6.4 Hz, 2H), 1.67 (s, 4H). ^{13}C NMR (100 MHz, $CDCl_3$) δ 169.8, 154.7, 144.8, 143.5, 139.6, 137.2, 137.1, 135.7, 135.0, 134.9, 134.5, 134.2, 133.2, 132.3, 131.6, 131.3, 129.9 (t, *J* = 248.6 Hz), 129.7, 128.4, 125.2, 65.0, 52.7 (td, *J* = 32.2 Hz, 12.0 Hz), 51.9 (d, *J* = 9.1 Hz), 43.6, 33.7 (dt, *J* = 45.6 Hz, 24.3 Hz), 26.2, 25.2 (d, *J* = 8.6 Hz), 21.0. HRMS (ESI): calcd for $C_{28}H_{26}Cl_2F_2N_3O_6S_2$, $[M-H]^-$ 672.0614, found 672.0608. HPLC purity: 96.69 %.

*4-Chloro-2-((4-((3,4-dichlorophenyl)thio)-N-(4-morpholinobutyl)-3-nitrophenyl)sulfonamido)benzoic acid (**10d**)*

Yellow solid (25 mg, 39 %). mp 163 – 165 °C. ^{1}H NMR (400 MHz, DMSO-d_6) δ 8.26 (d, *J* = 1.8 Hz, 1H), 8.02 (d, *J* = 1.9 Hz, 1H), 7.87 (d, *J* = 8.3 Hz, 1H), 7.67 (dd, *J* = 8.3, 1.9 Hz, 1H), 7.65 – 7.57 (m, 2H), 7.35 (d, *J* = 6.7 Hz, 1H), 7.12 (d, *J* = 8.6 Hz, 1H), 7.03 (d, *J* = 8.1 Hz, 1H), 3.80 (s, 4H), 3.61 (t, *J* = 6.1 Hz, 4H), 2.96 (s, 4H), 2.35 (s, 3H), 1.69 (s, 2H), 1.46 (s, 2H). ^{13}C NMR (100 MHz, DMSO-d_6) δ 167.4, 144.7, 142.8, 139.0, 137.2, 136.7, 136.0, 134.5, 133.4, 133.2, 133.1, 133.0, 132.4, 132.0, 130.8, 130.7,

130.0, 124.9, 63.8, 56.0, 51.5, 51.2, 25.7, 20.9, 20.6. HRMS (ESI): calcd for $C_{28}H_{28}Cl_2N_3O_7S_2$, $[M-H]^-$ 652.0751, found 652.0759. HPLC purity: 99.12 %.

4.2 Biology

4.2.1. Determination of minimum inhibitory concentration (MIC)

The antimicrobial activity of the compounds was determined by broth microdilution according to the Clinical and Laboratory Standards Institute (CLSI) guidelines [32]. The test medium was cation-adjusted Mueller-Hinton broth (CA-MHB) if not specified elsewhere or brain heart infusion (BHI) broth as indicated in the main text. Serial two-fold dilutions of the tested compound were performed for the tested chemicals starting from 256 μg/mL to 0.25 μg/mL, and the bacterial cell inoculum was adjusted to approximately 5×10^5 CFU per mL. Results were taken after 20-hour of incubation at 37°C. The MIC was defined as the lowest concentration of antibiotic with no visible growth. Experiments were performed in duplicates.

4.2.2. Determination of inhibitory activity to β'CH-σ interaction

Previously established protocols were used for inhibitor testing [38]. Protein overproduction and purification were performed as detailed previously [38]. C-SmBiT-CH (40 μL, 2.5 μM in PBS) was added to 96-well plates and then mixed with 20 μL of compound at desired concentrations. The mixture was incubated for 10 min at 37°C. C-LgBiT-σ^A (40 μL, 2.5 μM in PBS) was then added to each well, followed by incubation for 10 min at 37°C. After the final incubation step, an equal volume of Promega Nano-

Glo® Luciferase Assay Substrate (Promega, Madison, Wisconsin, United States) was added to the reaction mixture. Luminescence emitted was measured using a Victor X3 Multilabel plate reader (Waltham, Massachusetts, United States). Experiment was performed in triplicates with technical repeats for consistent results.

4.2.3. Epifluorescence microscopy

B. subtilis strain BS1048 [39] was grown on LB agar plate containing 5 μg/mL chloramphenicol and 0.5% (w/v) xylose. A single colony was incubated in LB medium mixed with 5 μg/mL chloramphenicol and 0.5% (w/v) xylose at 37°C until OD_{600} ~ 0.6. Chloramphenicol, rifampicin, or compound **5d** was then added to the culture and allowed to incubate for further 15 min. 2.5 μL of cell culture was placed onto 1.2% freshly made agarose plate and covered with a coverslip prior to imaging. Nikon eclipse Ti2-E live-cell fluorescence imaging system equipped with 60× /1.4 oil objective and LED illumination system were used to capture the fluorescence images. The fluorescence images were processed with Nikon NIS-Elements and MetaMorph software.

4.2.4. In vitro transcription assay

Transcription reactions were assembled in black 96 well plates. 16 nM E. coli RNAP mixed with σ^{70} (NEB) was incubated with 50 μM compounds (5d/7a/7c/10c) or rifampicin in 20 μL reactions at 37ºC for 10 min. RNA synthesis was initiated by adding 20 μL start solution of 10 nM pNG1299 and 1 mM rNTPs (NEB) at 37ºC for 15 min. Transcription was halted by adding 40 μL stop solution of 10 mM Tris-HCl pH 8.0, 1 mM EDTA, and 144 μM malachite green oxalate salt (Sigma), followed by signal

development on ice for 5 min. The fluorescence signal was read by a Synergy H1 plate reader (BioTek) with excitation at 620 nM and emission at 660 nM. Technical repeats were done for data reproducibility. One-way ANOVA was performed to measure the statistical significance. The data were represented in GraphPad Prism style. $p \leq 0.05$ (*), ≤ 0.01 (**), ≤ 0.001 (***), ≤ 0.0001 (****).

4.2.5. Molecular docking

Molecular docking of the compounds into β'CH extracted from *E. coli.* RNAP (PDB 4LJZ) was performed using AutoDock Vina. The AutoDock Tools-1.5.7 were used to prepare the ligands and macromolecule to generated PDBQT files. The binding pocket was defined with center of (8.242, -53.403, -46.042) and sizes of (13, 13, 13). Finally, the docking poses were visually prepared using PyMOL academic version (Schrödinger, LLC).

4.2.6. Cytotoxicity assay

Lung carcinoma A549 and hepatocellular carcinoma HaCaT cell lines were used to assess the cytotoxicity of antimicrobial compounds as described previously [10]. On Day 0, cells were seeded at 2.5×10^5 per well in a 96-well plate. Following 24 hrs overnight incubation at 37ºC, test compounds and the positive control cisplatin were added in two-fold serial dilutions ranging from 1.562 mg/mL to 50 µg/mL. Plates were then incubated at 37°C, and CCK-8 assay was performed at 48 hrs and 72 hrs following addition of compounds to determine cell viability. Results were presented as 50% cytotoxic concentration (CC_{50}) values alongside their respective standard deviations,

referring to the concentrations of compounds that reduced cell viability by 50% compared to untreated control.

4.2.7. Pharmacokinetic property prediction

Analysis of ADMET parameters such as water solubility, molar refractivity, topological polar surface area, Caco-2 cell permeability, intestinal absorption, the volume of distribution, fraction unbound, and ability to inhibit the P-glycoprotein of compounds **5d** and **7d** were studied using pkCSM. The SMILES files of compounds were generated by ChemDraw 22.0.0, then were input into pkCSM for generating the predicted values.

Acknowledgments

We gratefully acknowledge the financial support from the Research Grants Council of the Hong Kong Special Administrative Region, China (PolyU 15100021 and C5008-19G to C.M., CUHK 14107919 to X.Y.), Hong Kong Polytechnic University (1-ZE2E and the State Key Laboratory of Chemical Biology and Drug Discovery to C.M.), Hong Kong Food and Health Bureau HMRF (19180052 to X.Y.) and the Chinese University of Hong Kong (Faculty of Medicine Faculty Innovation Award FIA2018/A/03, and Passion for Perfection Scheme PFP202210-008 to X.Y.). We thank the University Research Facility in Life Sciences (ULS) of the Hong Kong Polytechnic University for the technical assistance.

Appendix A. Supplementary data

Supplementary data to this article can be found online at https://

Abbreviations

MRSA methicillin-resistant *Staphylococcus aureus*

VRSA vancomycin-resistant *Staphylococcus aureus*

PPI protein-protein interaction

MIC minimum inhibitory concentration

SAR structure-activity relationship

CD circular dichroism

QSAR quantitative structure-activity relationship

rRNA ribosomal RNA

DCM dichloromethane

THF tetrahydrofuran

DMSO dimethyl sulfoxide

References

[1] C. Ma, X. Yang, P.J. Lewis, Bacterial Transcription as a Target for Antibacterial Drug Development, Microbiol Mol Biol Rev 80(1) (2016) 139-60.
[2] A. Manten, L.J. van Wijngaarden, Development of drug resistance to rifampicin, Chemotherapy 14(2) (1969) 93-100.
[3] A.L. Sonenshein, H.B. Alexander, D.M. Rothstein, S.H. Fisher, Lipiarmycin-resistant ribonucleic acid polymerase mutants of Bacillus subtilis, J Bacteriol 132(1) (1977) 73-9.
[4] X. Yang, P.J. Lewis, The interaction between bacterial transcription factors and RNA polymerase during the transition from initiation to elongation, Transcription 1(2) (2010) 66-9.
[5] D.E. Scott, A.R. Bayly, C. Abell, J. Skidmore, Small molecules, big targets: drug discovery faces the protein-protein interaction challenge, Nat Rev Drug Discov 15(8) (2016) 533-50.
[6] R. Kahan, D.J. Worm, G.V. de Castro, S. Ng, A. Barnard, Modulators of protein-protein interactions as antimicrobial agents, RSC Chem Biol 2(2) (2021) 387-409.
[7] S.H. Kirsch, F.P.J. Haeckl, R. Muller, Beyond the approved: target sites and inhibitors of bacterial RNA polymerase from bacteria and fungi, Nat Prod Rep 39(6) (2022) 1226-1263.
[8] X. Yang, C. Ma, P.J. Lewis, Identification of inhibitors of bacterial RNA polymerase, Methods 86 (2015) 45-50.
[9] T.F. Tsang, Y. Qiu, L. Lin, J. Ye, C. Ma, X. Yang, Simple Method for Studying in Vitro Protein-Protein Interactions Based on Protein Complementation and Its Application in Drug Screening Targeting Bacterial Transcription, ACS Infect Dis 5(4) (2019) 521-527.
[10] X. Yang, M.J. Luo, A.C.M. Yeung, P.J. Lewis, P.K.S. Chan, M. Ip, C. Ma, First-In-Class Inhibitor of Ribosomal RNA Synthesis with Antimicrobial Activity against Staphylococcus aureus, Biochemistry 56(38) (2017) 5049-5052.
[11] Y. Qiu, S.T. Chan, L. Lin, T.L. Shek, T.F. Tsang, N. Barua, Y. Zhang, M. Ip, P.K. Chan, N. Blanchard, G. Hanquet, Z. Zuo, X. Yang, C. Ma, Design, synthesis and biological evaluation of antimicrobial diarylimine and -amine compounds targeting the interaction between the bacterial NusB and NusE proteins, Eur J Med Chem 178 (2019) 214-231.
[12] Y. Qiu, S.T. Chan, L. Lin, T.L. Shek, T.F. Tsang, Y. Zhang, M. Ip, P.K. Chan, N. Blanchard, G. Hanquet, Z. Zuo, X. Yang, C. Ma, Nusbiarylins, a new class of antimicrobial agents: Rational design of bacterial transcription inhibitors targeting the interaction between the NusB and NusE proteins, Bioorg Chem 92 (2019) 103203.
[13] Y. Qiu, C. Ma, HPLC, quantitative NMR and HRMS spectroscopic data of nusbiarylins as a new class of antimicrobial agents, Data Brief 29 (2020) 105313.
[14] A.J. Chu, Y. Qiu, R. Harper, L. Lin, C. Ma, X. Yang, Nusbiarylins Inhibit Transcription and Target Virulence Factors in Bacterial Pathogen Staphylococcus aureus, Int J Mol Sci 21(16) (2020).
[15] Y. Qiu, A.J. Chu, T.F. Tsang, Y. Zheng, N.M. Lam, K.S.L. Li, M. Ip, X. Yang, C. Ma, Synthesis and biological evaluation of nusbiarylin derivatives as bacterial rRNA synthesis inhibitor with potent antimicrobial activity against MRSA and VRSA, Bioorg Chem 124 (2022) 105863.
[16] J. Ye, X. Yang, C. Ma, Ligand-Based Drug Design of Novel Antimicrobials against Staphylococcus aureus by Targeting Bacterial Transcription, Int J Mol Sci 24(1) (2022).
[17] C. Ma, X. Yang, H. Kandemir, M. Mielczarek, E.B. Johnston, R. Griffith, N. Kumar, P.J. Lewis, Inhibitors of bacterial transcription initiation complex formation, ACS Chem Biol 8(9) (2013) 1972-80.

[18] A. Feklistov, B.D. Sharon, S.A. Darst, C.A. Gross, Bacterial sigma factors: a historical, structural, and genomic perspective, Annu Rev Microbiol 68 (2014) 357-76.
[19] X. Yang, C. Ma, P. Lewis, A vector system that allows simple generation of mutant Escherichia coli RNA polymerase, Plasmid 75 (2014) 37-41.
[20] C. Ma, X. Yang, P.J. Lewis, Bacterial Transcription Inhibitor of RNA Polymerase Holoenzyme Formation by Structure-Based Drug Design: From in Silico Screening to Validation, ACS Infect Dis 2(1) (2016) 39-46.
[21] E. Andre, L. Bastide, P. Villain-Guillot, J. Latouche, J. Rouby, J.P. Leonetti, A multiwell assay to isolate compounds inhibiting the assembly of the prokaryotic RNA polymerase, Assay Drug Dev Technol 2(6) (2004) 629-35.
[22] S. Hinsberger, K. Husecken, M. Groh, M. Negri, J. Haupenthal, R.W. Hartmann, Discovery of novel bacterial RNA polymerase inhibitors: pharmacophore-based virtual screening and hit optimization, J Med Chem 56(21) (2013) 8332-8.
[23] B. Bae, E. Davis, D. Brown, E.A. Campbell, S. Wigneshweraraj, S.A. Darst, Phage T7 Gp2 inhibition of Escherichia coli RNA polymerase involves misappropriation of sigma70 domain 1.1, Proc Natl Acad Sci U S A 110(49) (2013) 19772-7.
[24] J. Ye, A.J. Chu, R. Harper, S.T. Chan, T.L. Shek, Y. Zhang, M. Ip, M. Sambir, I. Artsimovitch, Z. Zuo, X. Yang, C. Ma, Discovery of Antibacterials That Inhibit Bacterial RNA Polymerase Interactions with Sigma Factors, J Med Chem 63(14) (2020) 7695-7720.
[25] J. Ye, A.J. Chu, L. Lin, S.T. Chan, R. Harper, M. Xiao, I. Artsimovitch, Z. Zuo, C. Ma, X. Yang, Benzyl and benzoyl benzoic acid inhibitors of bacterial RNA polymerase-sigma factor interaction, Eur J Med Chem 208 (2020) 112671.
[26] J. Ye, A.J. Chu, L. Lin, X. Yang, C. Ma, First-In-Class Inhibitors Targeting the Interaction between Bacterial RNA Polymerase and Sigma Initiation Factor Affect the Viability and Toxin Release of Streptococcus pneumoniae, Molecules 24(16) (2019).
[27] J. Ye, X. Yang, C. Ma, QSAR, Docking, and Molecular Dynamics Simulation Studies of Sigmacidins as Antimicrobials against Streptococci, Int J Mol Sci 23(8) (2022).
[28] E.A. Ilardi, E. Vitaku, J.T. Njardarson, Data-mining for sulfur and fluorine: an evaluation of pharmaceuticals to reveal opportunities for drug design and discovery, J Med Chem 57(7) (2014) 2832-42.
[29] R. Bernardez, J. Suarez, M. Fananas-Mastral, J.A. Varela, C. Saa, Tandem long distance chain-walking/cyclization via RuH2 (CO)(PPh3) 3/Brønsted acid catalysis: entry to aromatic oxazaheterocycles, Organic letters 18(4) (2016) 642-645.
[30] C. Ding, Q. Tian, J. Li, M. Jiao, S. Song, Y. Wang, Z. Miao, A. Zhang, Structural Modification of Natural Product Tanshinone I Leading to Discovery of Novel Nitrogen-Enriched Derivatives with Enhanced Anticancer Profile and Improved Drug-like Properties, J Med Chem 61(3) (2018) 760-776.
[31] WHO publishes list of bacteria for which new antibiotics are urgently needed. https://www.who.int/news/item/27-02-2017-who-publishes-list-of-bacteria-for-which-new-antibiotics-are-urgently-needed. (Accessed 8 June 2023).
[32] Clinical and Laboratory Standards Institute (CLSI), Performance Standards for Antimicrobial Susceptibility Testing, 33rd ed., Clinical and Laboratory Standards Institute, USA, 2023.
[33] H. Grundmann, M. Aires-de-Sousa, J. Boyce, E. Tiemersma, Emergence and resurgence of meticillin-resistant Staphylococcus aureus as a public-health threat, Lancet 368(9538) (2006) 874-85.
[34] N. Barua, L. Huang, C. Li, Y. Yang, M. Luo, W.I. Wei, K.T. Wong, N.W.S. Lo, K.O. Kwok, M. Ip, Comparative Study of Two-Dimensional (2D) vs. Three-Dimensional (3D) Organotypic Kertatinocyte-Fibroblast Skin Models for Staphylococcus aureus (MRSA) Infection, Int J Mol Sci 23(1) (2021).

[35] A.D. Khosravi, A. Jenabi, E.A. Montazeri, Distribution of genes encoding resistance to aminoglycoside modifying enzymes in methicillin-resistant Staphylococcus aureus (MRSA) strains, Kaohsiung J Med Sci 33(12) (2017) 587-593.
[36] J.I. Ross, E.A. Eady, J.H. Cove, S. Baumberg, Minimal functional system required for expression of erythromycin resistance by msrA in Staphylococcus aureus RN4220, Gene 183(1-2) (1996) 143-8.
[37] G.W. Kaatz, S.M. Seo, Inducible NorA-mediated multidrug resistance in Staphylococcus aureus, Antimicrob Agents Chemother 39(12) (1995) 2650-5.
[38] T.F. Tsang, Y. Qiu, L. Lin, J. Ye, C. Ma, X. Yang, Simple method for studying in vitro protein-protein interactions based on protein complementation and its application in drug screening targeting bacterial transcription, ACS Infect. Dis. 5(4) (2019) 521-527.
[39] P.J. Lewis, S.D. Thaker, J. Errington, Compartmentalization of transcription and translation in *Bacillus subtilis*, EMBO J. 19(4) (2000) 710-718.
[40] D.E. Pires, T.L. Blundell, D.B. Ascher, pkCSM: Predicting Small-Molecule Pharmacokinetic and Toxicity Properties Using Graph-Based Signatures, J Med Chem 58(9) (2015) 4066-72.
[41] M. Mielczarek, R.V. Devakaram, C. Ma, X. Yang, H. Kandemir, B. Purwono, D.S. Black, R. Griffith, P.J. Lewis, N. Kumar, Synthesis and biological activity of novel bis-indole inhibitors of bacterial transcription initiation complex formation, Org Biomol Chem 12(18) (2014) 2882-94.
[42] H. Kandemir, C. Ma, S.K. Kutty, D.S. Black, R. Griffith, P.J. Lewis, N. Kumar, Synthesis and biological evaluation of 2,5-di(7-indolyl)-1,3,4-oxadiazoles, and 2- and 7-indolyl 2-(1,3,4-thiadiazolyl)ketones as antimicrobials, Bioorg Med Chem 22(5) (2014) 1672-9.
[43] M. Mielczarek, R.V. Thomas, C. Ma, H. Kandemir, X. Yang, M. Bhadbhade, D.S. Black, R. Griffith, P.J. Lewis, N. Kumar, Synthesis and biological activity of novel mono-indole and mono-benzofuran inhibitors of bacterial transcription initiation complex formation, Bioorg Med Chem 23(8) (2015) 1763-75.
[44] O. Thach, M. Mielczarek, C. Ma, S.K. Kutty, X. Yang, D.S. Black, R. Griffith, P.J. Lewis, N. Kumar, From indole to pyrrole, furan, thiophene and pyridine: Search for novel small molecule inhibitors of bacterial transcription initiation complex formation, Bioorg Med Chem 24(6) (2016) 1171-82.
[45] D.S. Wenholz, M. Zeng, C. Ma, M. Mielczarek, X. Yang, M. Bhadbhade, D.S.C. Black, P.J. Lewis, R. Griffith, N. Kumar, Small molecule inhibitors of bacterial transcription complex formation, Bioorg Med Chem Lett 27(18) (2017) 4302-4308.
[46] C. Ma, M. Mobli, X. Yang, A.N. Keller, G.F. King, P.J. Lewis, RNA polymerase-induced remodelling of NusA produces a pause enhancement complex, Nucleic Acids Res 43(5) (2015) 2829-40.
[47] X. Yang, C. Ma, In Vitro Transcription Assays and Their Application in Drug Discovery, J Vis Exp (115) (2016).